

Effective field theory for deformed odd-mass nuclei

T. Papenbrock^{1,2} and H. A. Weidenmüller³

¹*Department of Physics and Astronomy, University of Tennessee, Knoxville, Tennessee 37996, USA*

²*Physics Division, Oak Ridge National Laboratory, Oak Ridge, Tennessee 37831, USA*

³*Max-Planck-Institut für Kernphysik, D-69029 Heidelberg, Germany*

We develop an effective field theory (EFT) for deformed odd-mass nuclei. These are described as an axially symmetric core to which a nucleon is coupled. In the coordinate system fixed to the core the nucleon is subject to an axially symmetric potential. Power counting is based on the separation of scales between low-lying rotations and higher-lying states of the core. In leading order, core and nucleon are coupled by universal derivative terms. These comprise a covariant derivative and gauge potentials which account for Coriolis forces and relate to Berry-phase phenomena. At leading order, the EFT combines the particle-rotor and Nilsson models. We work out the EFT up to next-to-leading order and illustrate the results in ²³⁹Pu and ¹⁸⁷Os. At leading order, odd-mass nuclei with rotational band heads that are close in energy and differ by one unit of angular momentum are triaxially deformed. For band heads that are well separated in energy, triaxiality becomes a subleading effect. The EFT developed in this paper presents a model-independent approach to the particle-rotor system that is capable of systematic improvement.

I. INTRODUCTION

In the last two decades, ideas based on effective field theory (EFT) and on the renormalization group have exerted a strong influence on nuclear-structure theory [1–6]. These ideas have led to model-independent approaches to nuclear interactions, currents, and nuclear spectra, to a new understanding of resolution-scale and scheme dependences in theoretical calculations [7–9], and to quantitative estimates of theoretical uncertainties [10, 11]. EFT exploits a separation of scale between the low-energy phenomena of interest and the excluded high-energy aspects. Thus, EFT can also be used to describe low-lying collective nuclear excitations such as rotations [12–18] and vibrations [19, 20]. Venerable nuclear collective models [21–23] have been identified as leading-order Hamiltonians in an EFT approach.

In this work, we develop an EFT for odd-mass deformed nuclei. These are viewed as a nucleon coupled to an axially symmetric core. Many even-even deformed nuclei exhibit some amount of triaxiality even in low-lying rotational bands. That, however, is often a small effect that can be treated as a higher-order correction to a first-order description that uses axial symmetry. Our approach differs from the general particle-rotor model and from a very recently developed EFT [18], both of which couple the nucleon to a triaxially deformed nucleus. As we will see below, the coupling of a nucleon to an axially symmetric core can, however, yield a triaxially deformed nucleus.

The theoretical arguments that lead to the Hamiltonian of the particle-rotor model are deceptively simple [24–28]: In the body-fixed (i.e. co-rotating) coordinate system (indicated here and in what follows by primes), a particle with angular momentum $\mathbf{K} = (K_{x'}, K_{y'}, K_{z'})$ is coupled to a rotor with angular momentum $\mathbf{R} = (R_{x'}, R_{y'}, R_{z'})$, resulting in the total angular momentum $\mathbf{I} = \mathbf{R} + \mathbf{K}$. The Hamiltonian of a rotor

is given by

$$H = \sum_{k=x',y',z'} \frac{R_k^2}{2C_k}. \quad (1)$$

Here, C_k are the moments of inertia. Replacing the components of \mathbf{R} by those of $\mathbf{I} - \mathbf{K}$ leads to the Hamiltonian

$$H_{\text{rot}} = \sum_{k=x',y',z'} \frac{(I_k - K_k)^2}{2C_k} \quad (2)$$

of the particle-rotor model. That model describes a wealth of data on odd-mass nuclei.

We are motivated to develop an EFT for the particle-rotor model because that approach is expected to yield a systematic classification of terms in the Hamiltonian according to their order of importance, with the Hamiltonian (2) expected to appear as the leading-order term. For that, the formulation of the particle-rotor model in terms of angular momenta is not a good starting point, however. In line with common usage, our EFT is based upon the Lagrangian or the Hamiltonian formalism. These, in turn, make use of velocities or canonical momenta, respectively. However, a Lagrangian approach to the particle-rotor system is not contained in the standard textbooks [21–23, 29–31].

In addition to providing a systematic procedure for generating Hamiltonian terms of given order, the EFT approach yields surprises and interesting results. For example, the coupling between the particle and the rotor can naturally be described in terms of Abelian and non-Abelian gauge potentials. Such potentials, and the Berry phases [32, 33] associated with them, enter in the description of diatomic molecules [34–36] and the quantum Hall effect [37]. However, Berry phases have received less attention in low-energy nuclear physics [38–43].

This paper is organized as follows. We identify the relevant low-energy degrees of freedom in Sect. II. In Sect. III we systematically construct the EFT by presenting the power-counting procedure and introducing

the relevant interactions at leading and at next-to-leading order. Hamiltonian and total angular momentum are introduced, the Hamiltonian is diagonalized and spectra in leading and subleading order are calculated in Section IV. We present applications of our results to ^{239}Pu and the triaxially deformed ^{187}Os in Sec. V, and summarize our results in Sect. VI. Numerous appendices give the technical details necessary for a self-contained description.

II. DEGREES OF FREEDOM AND SEPARATION OF SCALES

A. Even-even nucleus: rotating core

Many odd-mass deformed nuclei can be viewed as an even-even deformed nucleus to which the extra nucleon is coupled. We take ^{239}Pu as an example. The corresponding even-even nucleus is ^{238}Pu , and Fig. 1 shows all its levels below 800 keV. At sufficiently low energies the spectrum of ^{238}Pu is essentially that of an axially symmetric rigid rotor: The excitation energies $E(I)$ versus angular momentum I obey $E(I) = AI(I+1)$. Here A is a rotational constant of about 7 keV, and $\xi \approx 40$ keV (the energy of the $I = 2$ state) sets the low-energy scale. Only even spins enter because the ground state is invariant under rotations by π around any axis that is perpendicular to the symmetry axis. This symmetry is usually denoted as R symmetry [22]. At energy $\Lambda \approx 600$ keV a second rotational band with a $K^\pi = 1^-$ band head occurs, followed by more rotational bands at higher energies. In this work we will, however, consider only the lowest energies and restrict ourselves to the description of the ground-state rotational band. Then, the energy of the $K^\pi = 1^-$ band head sets the breakdown scale Λ of our EFT, because a new degree of freedom enters at this energy. We have a separation of scale $\xi \ll \Lambda$. The analysis of Ref. [44] shows that the ground-state band will exhibit noticeable deviations from the leading-order $E(I) = AI(I+1)$ rule for spins $I \gtrsim \Omega/\xi$. In the EFT this is due to subleading interactions that couple the ground-state band to other bands. While the interaction between the positive-parity ground-state band and the shown negative-parity band is suppressed, a positive-parity band enters at about 940 keV. These arguments suggest that the breakdown scale is properly chosen. An EFT for the lowest energies in deformed nuclei was presented in Refs. [12, 44], and we briefly review its essential features.

1. The rotor in quantum mechanics

Nuclear deformation causes an emergent breaking [45] of rotational symmetry from $\text{SO}(3)$ to axial $\text{SO}(2)$, described as a nonlinear realization of the symmetry [46–51]. The degrees of freedom corresponding to the remnants of Nambu-Goldstone bosons parametrize the coset

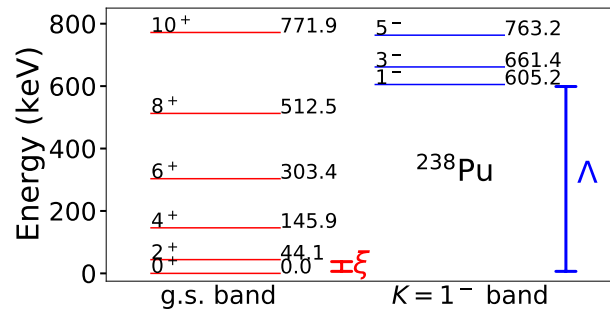


FIG. 1. (Color online) The levels of ^{238}Pu below 800 keV can be grouped in two rotational bands, with spin/parity and energy for each level as indicated. The low-energy scale $\xi \approx 40$ keV sets the scale for rotations. The breakdown scale $\Lambda \approx 600$ keV indicates a “vibrational” state, i.e. the breakdown of the axially-symmetric rigid-rotor picture for this nucleus.

$\text{SO}(3)/\text{SO}(2)$, i.e. the two-sphere. We use the radial unit vector

$$\mathbf{e}_r \equiv \cos \phi \sin \theta \mathbf{e}_x + \sin \phi \sin \theta \mathbf{e}_y + \cos \theta \mathbf{e}_z \quad (3)$$

for this purpose. Here, $(\mathbf{e}_x, \mathbf{e}_y, \mathbf{e}_z)$ are orthogonal unit vectors that span a right-handed coordinate system (the “space-fixed system”), and θ and ϕ are the polar and azimuthal angle, respectively. The vector \mathbf{e}_r in Eq. (3) points in the direction of the symmetry axis of the deformed nucleus. It is supplemented by the unit vectors

$$\begin{aligned} \mathbf{e}_\theta &\equiv \cos \phi \cos \theta \mathbf{e}_x + \sin \phi \cos \theta \mathbf{e}_y - \sin \theta \mathbf{e}_z, \\ \mathbf{e}_\phi &\equiv -\sin \phi \mathbf{e}_x + \cos \phi \mathbf{e}_y. \end{aligned} \quad (4)$$

The vectors $(\mathbf{e}_\theta, \mathbf{e}_\phi, \mathbf{e}_r)$ span the (right-handed) “body-fixed” coordinate system of the rotor. They result from rotating the axes \mathbf{e}_x , \mathbf{e}_y , and \mathbf{e}_z of the space-fixed system by the operator $\mathcal{R}(\phi, \theta, 0)$. Here \mathcal{R} stands for the general rotation

$$\mathcal{R}(\alpha, \beta, \gamma) \equiv e^{-i\alpha J_z} e^{-i\beta J_y} e^{-i\gamma J_z}, \quad (5)$$

parametrized in terms of the Euler angles (α, β, γ) . The operators J_k with $k = x, y, z$ generate rotations around the axes \mathbf{e}_k and fulfill the usual commutation relations

$$[J_x, J_y] = iJ_z \text{ (cyclic)}. \quad (6)$$

We also use the notation

$$\begin{aligned} \mathbf{e}'_x &= \mathbf{e}_\theta, \\ \mathbf{e}'_y &= \mathbf{e}_\phi, \\ \mathbf{e}'_z &= \mathbf{e}_r \end{aligned} \quad (7)$$

for the basis vectors of the body-fixed coordinate system.

In addition to the generators (J_x, J_y, J_z) of rotations in the space-fixed system we also use their analogues $(J_{x'}, J_{y'}, J_{z'})$ in the body-fixed system. These also obey the commutation relations (6). If space-fixed and body-fixed system originally coincide, the rotation (5) and the rotation

$$\mathcal{R}'(\alpha, \beta, \gamma) \equiv e^{-i\gamma J_{z'}} e^{-i\beta J_{y'}} e^{-i\alpha J_{x'}} \quad (8)$$

are identical [52]. For $\alpha = \phi$, $\beta = \theta$ the last two factors in expression (8) rotate the space-fixed z -axis into the direction of \mathbf{e}'_z . The remaining factor $e^{-i\gamma J_z}$ rotates the resulting system about the body-fixed \mathbf{e}'_z -axis. Hence, an operator defined in the body-fixed system that is invariant under SO(2) rotations, is automatically invariant under general SO(3) rotations in the space-fixed system. We use that insight to construct invariant terms in the Lagrangian.

Our definition (7) of the body-fixed coordinate system, resulting from the application of the rotation $\mathcal{R}(\phi, \theta, 0)$ to the space-fixed system, represents but one possibility. Any rotation $\mathcal{R}(\phi, \theta, \gamma)$ with $\gamma = \gamma(\theta, \phi)$ of the space-fixed system would be equally acceptable (albeit $\gamma = 0$ seems particularly simple). As we will see below, this arbitrary convention leads to a gauge freedom [53].

The time-dependent angles (θ, ϕ) describe the motion of the deformed nucleus. The angular velocity is

$$\begin{aligned} \mathbf{v} &\equiv \frac{d}{dt} \mathbf{e}_r \\ &= v_\theta \mathbf{e}_\theta + v_\phi \mathbf{e}_\phi, \end{aligned} \quad (9)$$

with

$$\begin{aligned} v_\theta &\equiv \dot{\theta}, \\ v_\phi &\equiv \dot{\phi} \sin \theta. \end{aligned} \quad (10)$$

The dot denotes the time derivative. We see that the rotor's degrees of freedom transform non-linearly [i.e. they depend in a nonlinear way on (ϕ, θ)] under the rotation. The expression \mathbf{v}^2 with \mathbf{v} defined in Eq. (9) is obviously invariant and so is, therefore, the Lagrangian

$$L_{\text{rot}} = \frac{C_0}{2} \mathbf{v}^2 = \frac{C_0}{2} (\dot{\theta}^2 + \dot{\phi}^2 \sin^2 \theta). \quad (11)$$

This is, of course, the Lagrangian of an axially symmetric rotor (or, equivalently, that of a particle on the unit sphere). Here C_0 is a low-energy constant and corresponds to the moment of inertia.

We introduce the canonical momenta $p_\theta = \partial L_{\text{rot}} / \partial \dot{\theta}$ and $p_\phi = \partial L_{\text{rot}} / \partial \dot{\phi}$ and perform a Legendre transform of the Lagrangian (11). This yields the Hamiltonian

$$H_{\text{rot}} = \frac{1}{2C_0} \left(p_\theta^2 + \frac{p_\phi^2}{\sin^2 \theta} \right) = \frac{\mathbf{p}^2}{2C_0}. \quad (12)$$

Here, we combined the canonical momenta into

$$\mathbf{p} \equiv p_\theta \mathbf{e}_\theta + \frac{p_\phi}{\sin \theta} \mathbf{e}_\phi. \quad (13)$$

We quantize the momentum \mathbf{p} as usual,

$$\mathbf{p} = -i\nabla_\Omega, \quad (14)$$

with

$$\nabla_\Omega \equiv \mathbf{e}_\theta \partial_\theta + \frac{\mathbf{e}_\phi}{\sin \theta} \partial_\phi. \quad (15)$$

The spectrum is

$$E(I) = \frac{I(I+1)}{2C_0}, \quad (16)$$

with angular momenta I , corresponding to a rotational band.

An alternative derivation of the rotor spectrum uses the angular momentum

$$\mathbf{I} = \mathbf{e}_r \times \mathbf{p}, \quad (17)$$

rewrites, $\mathbf{p} = -\mathbf{e}_r \times \mathbf{I}$ (which implies $\mathbf{p}^2 = \mathbf{I}^2$), and thereby obtains the Hamiltonian $\mathbf{I}^2 / (2C_0)$. We will use such an approach below.

2. Connection to effective field theory

The arguments in Section II.A.1 may seem purely phenomenological. We now establish the connection to EFT. For nonrelativistic quantum systems, that approach is summarized in Ref. [51], see also Ref. [49]. A paradigmatic application is that to the infinitely extended ferromagnet (FM) (Refs. [54–57]). The breaking of a symmetry of the Hamiltonian in the ground state of the system (in the FM: the common direction of all spins violates rotational invariance) causes the existence of Nambu-Goldstone modes (in the FM: spin waves). These make up for the fact that the FM cannot rotate. They determine the low-lying part of the spectrum of the FM, are determined entirely by the broken symmetry, and depend upon a small number of parameters that must be fitted to the data. In atomic nuclei, that EFT scheme must be generalized as we deal with “emergent symmetry breaking”, see Refs. [13, 14, 45]. In the limit of infinite mass, nuclei cannot rotate either. The Nambu-Goldstone modes are surface vibrations. Finite nuclei are able to undergo rotations, however. The associated degrees of freedom are the purely time-dependent angles $\theta(t)$ and $\phi(t)$ introduced in Section II.A.1. These degrees of freedom are not Nambu-Goldstone modes as they cease to carry physical significance in the infinite-mass limit. Rather they represent the onset of symmetry breaking in the finite system (hence “emergent symmetry breaking”). That approach is expected to work for systems close to full symmetry breaking. Then the relevant energy scales are (in increasing order) the rotational energy (via the degrees of freedom θ and ϕ), the surface vibrations (described in terms of Nambu-Goldstone modes), and genuine intrinsic excitations of the system (not accessible in terms of Nambu-Goldstone modes). In Refs. [13, 14] that approach has been worked out in detail for even-mass nuclei. In the present paper we confine ourselves in the description of the core to the very lowest part of the excitation spectrum, i.e., to rotations.

Needless to say we may re-formulate the quantum mechanics of the axially symmetric rotor as a quantum field theory. Based on the familiar rotor Hamiltonian (12) we

introduce the quantum field operator $\hat{\Phi}(\theta, \phi)$ that fulfills the canonical commutation relations for bosons

$$\left[\hat{\Phi}(\theta, \phi), \hat{\Phi}^\dagger(\theta', \phi') \right] = \delta(\phi - \phi') \delta(\cos \theta - \cos \theta'). \quad (18)$$

Here, $\hat{\Phi}^\dagger(\theta, \phi)$ creates an axially symmetric rotor whose symmetry axis points into the direction of \mathbf{e}_r .

The Lagrangian of the free rotor is then

$$L = \int_0^{2\pi} d\phi \int_{-1}^1 d \cos \theta \hat{\Phi}^\dagger(\theta, \phi) \left(i\partial_t + \frac{\nabla_\Omega^2}{2C_0} \right) \hat{\Phi}(\theta, \phi). \quad (19)$$

Introducing the momentum operator

$$\hat{\Pi}_\Phi(\theta, \phi) \equiv \frac{\delta L}{\delta \partial_t \hat{\Phi}(\theta, \phi)} = i\hat{\Phi}^\dagger(\theta, \phi) \quad (20)$$

and performing the usual Legendre transformation then yields the Hamiltonian

$$H = -\frac{1}{2C_0} \int_0^{2\pi} d\phi \int_{-1}^1 d \cos \theta \hat{\Phi}^\dagger(\theta, \phi) \nabla_\Omega^2 \hat{\Phi}(\theta, \phi). \quad (21)$$

This clearly is the second-quantized version of the Hamiltonian (12).

Although we are dealing with the rotor in quantum mechanics and not in quantum field theory we continue to use the terminology of EFT. This is in keeping with many works in low-energy nuclear physics where the ideas of EFTs [58] are used to construct and solve Hamiltonians in quantum mechanics, see, e.g., Refs. [59–63].

B. Nucleon

To gain insight into how to construct the EFT, we consider the odd-mass nucleus ^{239}Pu . Figure 2 shows all levels below 800 keV that can be grouped into rotational bands (omitting the few exceptions). The ground-state rotational band is built on a $K^\pi = \frac{1}{2}^+$ state, i.e., a $K^\pi = \frac{1}{2}^+$ neutron coupled to the ^{238}Pu ground state. Rotations of this nucleon-nucleus state then produce the rotational band on top of the $1/2^+$ ground state. The first excited neutron state yields the $K^\pi = \frac{5}{2}^+$ state at $\Omega \approx 300$ keV, and its rotations produce the corresponding rotational bands. Thus, the fermion single-particle excitation energy is about half the breakdown scale in this nucleus, and the condition $\Omega \ll \Lambda$ is fulfilled only marginally. The $K^\pi = \frac{1}{2}^-$ band head at about 470 keV could be due either to a single-neutron excitation or to the coupling of the $K^\pi = \frac{1}{2}^+$ neutron with the excited 1^- state (at the breakdown energy Λ) in ^{238}Pu . Therefore, that rotational band is beyond the breakdown scale of the EFT we present in this paper.

The rotational bands depicted in Fig. 2 all follow the pattern

$$E(I, K) = E_0 + A \left[I(I+1) + a\delta_{K,1/2}(-1)^{I+\frac{1}{2}} \left(I + \frac{1}{2} \right) \right]. \quad (22)$$

Here, E_0 is an energy offset, A the rotational constant, and a the decoupling parameter (that occurs only for $K = \frac{1}{2}$ bands). These constants depend on the band under consideration. Typically, we have $E_0 \sim \Omega$, $A \sim \xi/6$, and $a \sim \mathcal{O}(1)$. Equation (22) is well known from a variety of models [22, 23, 29, 31, 64]. As shown below, it is also the leading-order result of the EFT we develop in this paper.

We use the insight gained in the previous Subsection and request that the Lagrangian of the nucleon be invariant under SO(2) rotations in the body-fixed system. That guarantees invariance under SO(3) rotations in the space-fixed system.

The field operator $\hat{\psi}_s(\mathbf{x}')$ creates a fermion at position \mathbf{x}' with spin projection $s = \pm \frac{1}{2}$ onto the z' -axis in the body-fixed frame. Denoting the vacuum as $|0\rangle$ we thus have

$$\hat{\psi}_s^\dagger(\mathbf{x}')|0\rangle = \chi_{\frac{1}{2}s}|\mathbf{x}'\rangle. \quad (23)$$

Here $\chi_{\frac{1}{2}s}$ denotes a spin state of spin- $\frac{1}{2}$ fermion with z' projection s [52], and $|\mathbf{x}'\rangle$ is an eigenstate of the position operator. The corresponding annihilation operator is $\hat{\psi}_s(\mathbf{x}')$ and we have the usual anti-commutation relation for fermions

$$\left\{ \hat{\psi}_s(\mathbf{x}'), \hat{\psi}_\sigma^\dagger(\mathbf{y}') \right\} = \delta_\sigma^s \delta(\mathbf{x}' - \mathbf{y}'), \quad (24)$$

and all other anti commutators vanish. It will be useful to combine the two spin components of the field operator into the spinor

$$\hat{\Psi}(\mathbf{x}') \equiv \begin{pmatrix} \hat{\psi}_{+\frac{1}{2}}(\mathbf{x}') \\ \hat{\psi}_{-\frac{1}{2}}(\mathbf{x}') \end{pmatrix}. \quad (25)$$

The nucleon Lagrangian is

$$L_\Psi = \int d^3\mathbf{x}' \hat{\Psi}^\dagger(\mathbf{x}') \left(i\partial_t + \frac{\hbar^2 \Delta'}{2m} - V \right) \hat{\Psi}(\mathbf{x}'). \quad (26)$$

Here, V is an axially symmetric potential which may also depend on spin, i.e., be a 2×2 matrix. The potential of the Nilsson model [27] is an example. The Lagrangian (26) exhibits axial symmetry. The construction (26) is not only mandated by the nonlinear realization of rotational symmetry [12]. It is also consistent with an adiabatic approach where the light nucleon is much faster than the heavy and slowly rotating core and able to follow the core's motion quasi instantaneously. The canonical momentum is

$$\hat{\Pi}(\mathbf{x}') = \frac{\delta L}{\delta \partial_t \hat{\Psi}(\mathbf{x}')} = i\hat{\Psi}^\dagger(\mathbf{x}'). \quad (27)$$

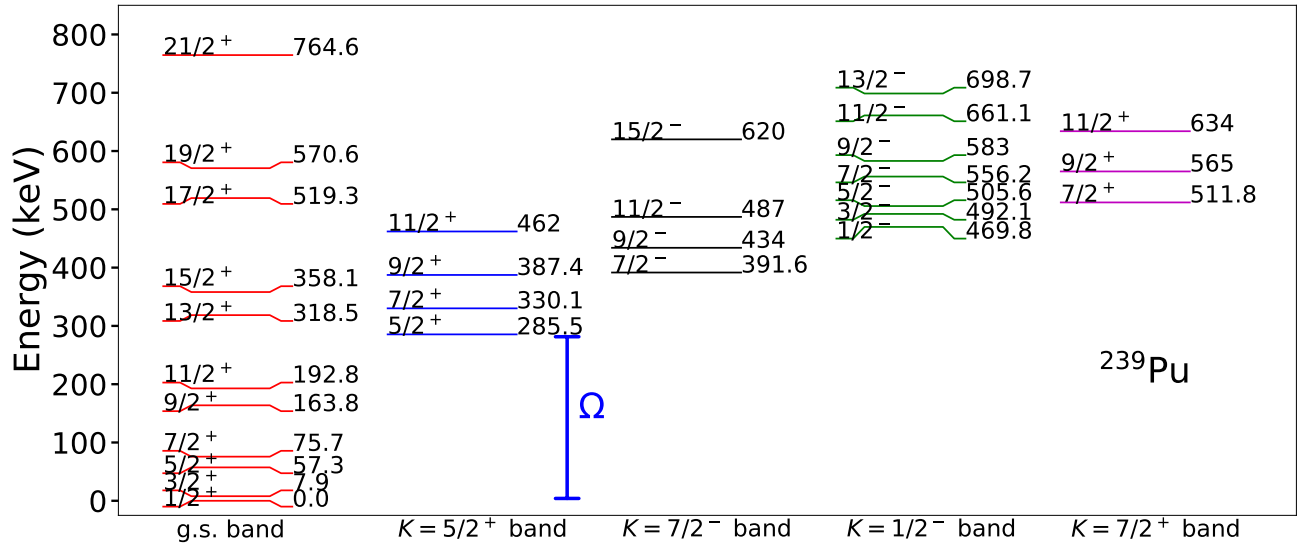


FIG. 2. (Color online) Levels of ^{239}Pu below 800 keV that can be grouped into rotational bands, with spins, parities, and energies as indicated. The energy $\Omega \approx 300$ keV sets the scale for single-particle excitations.

The Legendre transform of the Lagrangian (26) yields the Hamiltonian

$$H_\Psi = \int d^3\mathbf{x}' \hat{\Psi}^\dagger(\mathbf{x}') \left(-\frac{\hbar^2 \Delta'}{2m} + V \right) \hat{\Psi}(\mathbf{x}'). \quad (28)$$

Here, we introduced the Laplacian $\Delta' = \nabla' \cdot \nabla'$. The total angular momentum of the fermion,

$$\mathbf{K} = \int d^3\mathbf{x}' \hat{\Psi}^\dagger(\mathbf{x}') \left(-i\mathbf{x}' \times \nabla' + \hat{\mathbf{S}} \right) \hat{\Psi}(\mathbf{x}'), \quad (29)$$

is the sum of orbital angular momentum and spin

$$\hat{\mathbf{S}} = \frac{1}{2} \begin{pmatrix} \sigma_{x'} \\ \sigma_{y'} \\ \sigma_{z'} \end{pmatrix}. \quad (30)$$

Here, $\sigma_{x'}, \sigma_{y'}, \sigma_{z'}$ denote the usual Pauli matrices. These act with respect to the axes of the body-fixed system. The action of the general operators ($J_{x'}, J_{y'}, J_{z'}$) on the space- and spin-degrees of freedom of the nucleon coincides with that of the corresponding angular momentum plus spin operators in Eq. (29). Thus, for $k' = x', y', z'$,

$$K_{k'} \equiv \mathbf{e}'_{k'} \cdot \mathbf{K} = \int d^3\mathbf{x}' \hat{\Psi}^\dagger(\mathbf{x}') J_{k'} \hat{\Psi}(\mathbf{x}') \quad (31)$$

are the projections of the fermion's angular momentum onto the body-fixed axes.

Fermion states of axially-symmetric Hamiltonians H_Ψ are written as $|K, \alpha\rangle$. Here K denotes the projection of the angular momentum onto the nuclear symmetry axis, while α comprises the remaining quantum numbers energy, parity, and third component of isospin. Kramers' degeneracy (i.e., time-reversal invariance) implies that the single-Fermion states come in degenerate pairs $|\pm K, \alpha\rangle$, carrying identical quantum numbers α

and, in particular, sharing the same energy $E_{|K|, \alpha}$. Thus, we have

$$\begin{aligned} H_\Psi |K, \alpha\rangle &= E_{|K|, \alpha} |K, \alpha\rangle, \\ \hat{K}_{z'} |K, \alpha\rangle &= K |K, \alpha\rangle. \end{aligned} \quad (32)$$

We understand the band heads in Fig. 2 simply as energy eigenvalues of the fermion Hamiltonian H_Ψ with a suitably chosen potential V . The R symmetry of the nuclear ground state ensures that only a suitable linear combination of the states $|\pm K, \alpha\rangle$ enters. The energies $E_{|K|, \alpha}$ of the band heads are of the scale Ω . Thus, if we had spontaneous rather than emergent symmetry breaking, $\xi \rightarrow 0$ would hold, and the rotational bands on top of each band head would collapse.

The degrees of freedom of the rotor do not appear explicitly in Eq. (28). Conversely, the potential V has no impact on the degrees of freedom of the rotor. The potential V constitutes an implicit interaction between the rotor and the particle which is solely based on the fact that the potential is axially symmetric and defined in the body-fixed frame. That is consistent with emergent symmetry breaking which allows only a coupling to derivatives of Nambu-Goldstone bosons, in our case: the angular velocity. Such interactions – not yet contained in the Hamiltonian (28) – will appear as gauge couplings of the nucleon to the rotor. These are partly constrained by the nonlinear realization of rotational symmetry. They appear in universal form as a covariant derivative or as Coriolis terms. They can also be understood within an adiabatic approach that involves Berry phases.

III. BUILDING AN EFFECTIVE FIELD THEORY

Having identified in Section II the relevant degrees of freedom due to a separation of scales, we now construct our effective field theory for odd-mass deformed nuclei using the following steps. (i) In the present Section we define the power-counting procedure and (ii) write down the interaction terms between the nucleon and the rotor in leading and some also in subleading order. In step (ii) all possible interaction terms are admitted that are allowed by the symmetries (in our case invariance under rotations, parity, and time reversal), see, e.g., Ref. [51]. (iii) The resulting Lagrangian and Hamiltonian, further subleading terms, and the solution of the equations of motion are addressed in Section IV.

A. Power counting

The power-counting procedure for the rotor was worked out in Refs. [12, 13]. We briefly present the arguments. We associate the low-energy scale ξ with the rotor. Thus, the angular velocity scales as ξ ,

$$\begin{aligned} |\mathbf{v}| &\sim \xi, \\ \dot{\theta} &\sim \xi, \\ \dot{\phi} &\sim \xi, \end{aligned} \quad (33)$$

and so does the Lagrangian (11) of the free rotor. That implies that its low-energy constant scales as

$$C_0 \sim \xi^{-1}. \quad (34)$$

The spectrum of the free axially symmetric rotor forms a rotational band, see Eq. (16), and C_0 is the moment of inertia. Let us give examples. $C_0^{-1} \approx 1$ MeV for a light rotor such as ${}^8\text{Be}$, 0.5 MeV in ${}^{24}\text{Mg}$, 0.2 MeV in the neutron-rich nucleus ${}^{34}\text{Mg}$, 30 keV for a rare earth nucleus, and only 15 keV for actinides. These are the smallest energy scales in the nuclei we consider. The breakdown energy Λ for the rotor is set by excitations that are not part of its ground-state rotational band. This energy is about 17 MeV in ${}^8\text{Be}$, 4 MeV in ${}^{24}\text{Mg}$, 1 MeV in rare earth nuclei, and about 0.5 MeV in actinides. Thus, $\Lambda \gg \xi$ in all cases.

The subleading correction to the rotor Lagrangian (11) is

$$C_2(\mathbf{v}^2)^2. \quad (35)$$

At the breakdown scale, i.e., when $|\mathbf{v}| \sim \Lambda$, the term (35) is by definition equal in importance to the leading-order Lagrangian (11). That yields

$$C_2 \sim \xi^{-1}\Lambda^{-2}. \quad (36)$$

At low energy where $|\mathbf{v}| \sim \xi$, the term (35) yields a contribution $\sim \xi^3/\Omega^2$ to the total Lagrangian, and this is suppressed by $\xi^2/\Omega^2 \ll 1$ compared to the leading term (11).

That argument establishes the power-counting procedure for the rotor: the energy scale ξ is associated with rotational bands. Corrections to the leading-order term come in powers of ξ/Λ .

We turn to the energy scales of the Hamiltonian (28) of the nucleon. The energy scale Ω is set by the mean level spacing of the single-nucleon states, i.e., by the spacing of band-head energies $E_{|K|\alpha}$ in odd-mass nuclei, see Eq. (32). That scale is about 1.7 MeV in ${}^9\text{Be}$, (given by the energy difference of the $3/2^-$ ground state and the excited $1/2^+$ band head), 0.6 MeV in ${}^{25}\text{Mg}$, (given by the energy difference between the $5/2^+$ ground state and the excited $1/2^+$ band head), and amounts to some hundreds of keV in rare earth nuclei, and to tens to hundreds of keV for actinides. In most odd-mass deformed nuclei we have $\Omega \gtrsim \xi$, and in many cases one even finds $\Omega \gg \xi$, see ${}^{239}\text{Pu}$ in Fig. 2 as an example. In such cases Ω is only about a factor two or three away from the breakdown scale Λ , and the separation between Ω and Λ is marginal so that $\Omega \lesssim \Lambda$ but not $\Omega \ll \Lambda$. In such cases, the power counting uses both small expansion parameters ξ/Λ and ξ/Ω , and it is difficult to decide which is the more important one. If we had the ambition to construct an EFT for the nucleon potential in the Hamiltonian (28) we would have to deal, in addition, with an expansion in powers of Ω/Λ , but we do not pursue this task in the present paper. In some nuclei such as ${}^{187}\text{Os}$ discussed below, we have $\Omega \sim \xi$ so that $\xi, \Omega \ll \Lambda$. Then, the power counting is in ξ/Λ . [We avoid the equivalent parameter Ω/Λ as that might incorrectly suggest a systematic expansion of the nucleon potential in the Hamiltonian (28).]

In any case, the separation of scales allows us to construct an EFT that systematically improves the energies and states in rotational bands. We note that there are many states in odd-mass nuclei that do not result from coupling a nucleon to the ground-state band of the even-even nucleus (but rather from coupling to excited band heads of the even-even nucleus). Such states fall outside the purview of the EFT we aim to construct. Including such effects would require us to introduce fields that describe the non-rotational excitations of the rotor.

It would be desirable to construct the potential V in the fermion Hamiltonian (28) in a similarly systematic fashion. We briefly illuminate the difficulties in doing so for halo rotors, i.e., odd-mass nuclei where the nucleon is weakly bound to the even-even core. Examples are ${}^9\text{Be}$ (with a neutron separation energy of about 1.7 MeV) and neutron-rich magnesium isotopes with separation energies below 1 MeV. In these cases, the fermion's de-Broglie wave length exceeds the rotor's size, and a derivative expansion of the potential seems appropriate. The potential V must be axially symmetric. Total spin $\hat{\mathbf{S}}^2 = 3/4$ and its projection $\hat{S}_z^2 = 1/4$ are trivial constants, while \hat{K}_z is the nontrivial conserved quantity and can be used to classify the fermion's wave functions. Thus, we can

parameterize the potential as

$$\begin{aligned}
V = & v_{01}\delta(\mathbf{r}') \\
& + v_{11}\nabla_{\perp}\delta(\mathbf{r}')\cdot\nabla_{\perp} + v_{12}\partial_{z'}\delta(\mathbf{r}')\partial_{z'} \\
& + v_{13}\left[\nabla_{\perp}^2\delta(\mathbf{r}') + \delta(\mathbf{r}')\nabla_{\perp}^2\right] \\
& + v_{14}\left[\partial_{z'}^2\delta(\mathbf{r}') + \delta(\mathbf{r}')\partial_{z'}^2\right] \\
& + v_{15}(\hat{\sigma}_{x'}\partial_{x'} + \hat{\sigma}_{y'}\partial_{y'})\delta(\mathbf{r}')(\hat{\sigma}_{x'}\partial_{x'} + \hat{\sigma}_{y'}\partial_{y'}) \\
& + v_{16}\left[(\hat{\sigma}_{x'}\partial_{x'} + \hat{\sigma}_{y'}\partial_{y'})\hat{\sigma}_{z'}\partial_{z'}\delta(\mathbf{r}') \right. \\
& \quad \left. + \delta(\mathbf{r}')\hat{\sigma}_{z'}\partial_{z'}(\hat{\sigma}_{x'}\partial_{x'} + \hat{\sigma}_{y'}\partial_{y'})\right] \\
& + \dots .
\end{aligned} \tag{37}$$

Here, $\nabla_{\perp} \equiv r^{-1}\nabla_{\Omega}$. In Eq. (37) we did not present all second-order derivatives, and higher-order derivatives are missing as well. If the fermion has quantum numbers $J^{\pi} = \frac{1}{2}^{+}$, the leading-order contribution consists solely of the v_{01} contact coupling. For $J^{\pi} = \frac{3}{2}^{-}$ or $\frac{1}{2}^{-}$ states (e.g. for the ground state and excited band head at about 2.8 MeV, respectively, in ${}^9\text{Be}$), second-order derivatives in the potential V must enter. In the latter case, one also needs to employ a potential that breaks spherical symmetry down to axial symmetry, thus lifting the four-fold degeneracy of a $p_{3/2}$ orbital in the body-fixed frame. The considerable number of low-energy coefficients then requires that a significant amount of data is available. In practice, one would like to adjust to scattering data (and make predictions for spectra and transitions), but those are rare. Odd-mass neutron-rich isotopes of magnesium, for instance, are expected to have $\frac{5}{2}^{+}$ ground states. This would require us to carry the expansion (37) to even higher order, and the scarcity of data in rare isotopes would prohibit us to follow such an EFT approach. It is, therefore, more practical to assume that the Hamiltonian (28) is already in diagonal form, with low-energy eigenstates as given in Eq. (32) fitted to the data. In other words, we take the single-particle energies of the fermion from data. This is somewhat similar in spirit to halo EFT [6] where each state of the core is represented as a separate field and simply adjusted to data.

The resulting EFT involves – in leading order – terms of order ξ and Ω . Subleading corrections are suppressed by factors of ξ/Λ (or ξ/Ω provided that $\xi \ll \Omega$ holds). This EFT does not provide us with an expansion in powers of Ω/Λ , because we do not construct such an expansion of the potential V .

B. Nucleon-rotor interactions

We deal with emergent symmetry breaking. Thus, the nucleon can couple to the rotor only derivatively, i.e., via the angular velocity \mathbf{v} . All terms allowed by the symmetries must be considered. At face value, the resulting velocity-dependent couplings are well known. They involve – in the body-fixed frame – Coriolis forces. However, the essential physical argument for the couplings is more subtle and profound. The coupling terms are

gauge couplings that involve Berry phases (or geometrical phases). Such phases occur in many quantum systems [32, 33]. While originally conceived for systems that undergo a time-dependent adiabatic motion, they may also occur where “fast” degrees of freedom have been removed or integrated out, and where one is only interested in the remaining “slow” degrees of freedom [65]. A well-known example from molecular physics is the Born-Oppenheimer approximation. Here, Berry phases and the corresponding gauge potentials enter the dynamics of the nuclei of the molecule once the electronic degrees of freedom have been removed. That leads to the molecular Aharonov-Bohm effect [34, 66]. For the diatomic molecule, some details are presented in Refs. [35, 36, 67]. In the present case, the fact that the nucleon is much faster than the slowly rotating core shows that gauge potentials play a role. Likewise, gauge potentials are a general feature of systems where a separation between rotational and intrinsic degrees of freedom is being made, and different conventions for this separation differ by gauge transformations [53].

The non-linear realization of rotational invariance requires that, in the body-fixed system, we have to replace the time derivative $i\partial_t$ in the Lagrangian (26) by the covariant derivative [12] (see Appendices C and D)

$$iD_t \equiv i\partial_t + \dot{\phi} \cos\theta [J_{z'}, \cdot] . \tag{38}$$

Here, the commutator’s second argument is left open. The last term of the covariant derivative accounts for Coriolis effects in the body-fixed system. It is present even if the Lagrangian in the body-fixed system does not depend on time explicitly, i.e., even if the partial time derivative vanishes. In the Lagrangian (26) that yields

$$\begin{aligned}
& \int d^3\mathbf{x}' \hat{\Psi}^{\dagger}(\mathbf{x}') iD_t \hat{\Psi}(\mathbf{x}') \\
& = \int d^3\mathbf{x}' \hat{\Psi}^{\dagger}(\mathbf{x}') i\partial_t \hat{\Psi}(\mathbf{x}') + \mathbf{v} \cdot \left(\mathbf{e}_{\phi} \cot\theta \hat{K}_{z'} \right) .
\end{aligned} \tag{39}$$

We have factored out the angular velocity \mathbf{v} , see Eq. (9), and we have used Eq. (31). This naturally introduces the gauge potential

$$\mathbf{A}_a(\theta, \phi) \equiv \mathbf{e}_{\phi} \cot\theta \hat{K}_{z'} \tag{40}$$

which couples the rotor to the nucleon via $\mathbf{v} \cdot \mathbf{A}_a$. Here we borrow the expression gauge potential from electrodynamics. In the parlance of differential geometry, the field \mathbf{A}_a is a connection. The term $\mathbf{v} \cdot \mathbf{A}_a$ scales as ξ , i.e. the gauge potential is dimensionless and of order one. Thus, the gauge term is as important as the Lagrangian (11) of the free rotor and enters in leading order.

The gauge potential (40) is singular at the north and south poles of the unit sphere. Single-valuedness of the wave function for the rotor requires that the eigenvalues K of $\hat{K}_{z'}$ be integer or half integer. That is obviously guaranteed for the fermion for which $K = \pm\frac{1}{2}, \pm\frac{3}{2}, \dots$. We compute the corresponding magnetic field (or the Berry curvature in differential geometry) and find

$$\mathbf{B}_a(\theta, \phi) \equiv \nabla_{\Omega} \times \mathbf{A}_a = -\mathbf{e}_r \hat{K}_{z'} . \tag{41}$$

This is the field of a Dirac monopole on the unit sphere and clearly exhibits spherical symmetry [68, 69], in contrast to the gauge potential (40) whose rotational invariance is not obvious. As shown in App. E2, the effect of a rotation on the gauge potential (40) can be reversed by a gauge transformation.

To see that the field (41) is indeed a monopole field we take a detour and consider a sphere of radius R of the size of the nucleus, with angular and radial coordinates (θ, ϕ) and ρ , respectively. We neglect excitations of the sphere in the radial direction as these relate to vibration with energies at the breakdown scale and put $\rho = R$. Then angular velocities and the vector potential (40) are multiplied with R and R^{-1} , respectively. The usual differential operator $\mathbf{e}_r \partial_R + R^{-1} \nabla_\Omega$ then shows that we deal indeed with a monopole field.

The gauge potential (40) is intimately linked to the geometry of the sphere, i.e. the coset space $\text{SO}(3)/\text{SO}(2)$. To see this, we consider a sequence of three rotations (around space-fixed axes) that take the rotor from a point A on the unit sphere to a point B , then from B to a point C , and finally from point C back to the point A . We assume that the three rotations are around three distinct axes. This ensures that the triangle ABC on the sphere has a finite solid angle (or area). It is clear that at least two of the three rotations will also induce rotations of the fermion field around the body-fixed z' -axis. While the rotor has returned to its original configuration after the sequence of the three rotations, the fermion's configuration has been changed by a finite rotation around the body-fixed z' -axis. Inspection shows that the rotation angle, i.e. the phase acquired by the fermion with spin projection K , is equal to the solid angle of the enclosed loop times the spin projection K . Dynamically this phase is acquired because of the monopole magnetic field.

Another gauge coupling, permitted in the framework of our EFT, is

$$g\mathbf{v} \cdot (\mathbf{e}_r \times \mathbf{K}) . \quad (42)$$

Here, g is a dimensionless coupling constant. Its natural size is of order unity, and the contribution (42) scales as ξ and enters at leading order. The corresponding gauge potential is

$$\mathbf{A}_n(\theta, \phi) = g\mathbf{e}_r \times \mathbf{K} = g \left(\mathbf{e}_\phi \hat{K}_{x'} - \mathbf{e}_\theta \hat{K}_{y'} \right) . \quad (43)$$

This vector potential contains non-commuting operators and, therefore, constitutes a non-Abelian gauge potential. The corresponding magnetic field is

$$\begin{aligned} \mathbf{B}_n(\theta, \phi) &\equiv \nabla_\Omega \times \mathbf{A}_n - i\mathbf{A}_n \times \mathbf{A}_n \\ &= g\mathbf{e}_r \cot \theta \hat{K}_{x'} + g^2 \mathbf{e}_r \hat{K}_{z'} . \end{aligned} \quad (44)$$

Taken by itself, this magnetic field is not invariant under rotations. However, the total gauge potential is

$$\mathbf{A}_{\text{tot}} = \mathbf{A}_a + \mathbf{A}_n , \quad (45)$$

and the corresponding magnetic field

$$\begin{aligned} \mathbf{B}_{\text{tot}} &\equiv \nabla_\Omega \times \mathbf{A}_{\text{tot}} - i\mathbf{A}_{\text{tot}} \times \mathbf{A}_{\text{tot}} \\ &= (g^2 - 1)\mathbf{e}_r \hat{K}_{z'} \end{aligned} \quad (46)$$

is spherically symmetric. Again, we deal with a magnetic monopole. However, in contrast to the field (41) its overall strength is not quantized because the non-Abelian vector potential (43) exhibits no singularities on the unit sphere and the coupling g can therefore assume any real value.

To show how this gauge term relates to the Berry phase we observe that the states $|\pm K, \alpha\rangle$ have the same energy, see Eq. (32). When the rotor moves along a closed loop on the unit sphere, a general interaction would mix the two degenerate states while transversing the loop. Thus, the initial and final fermion states could differ by a unitary transformation. The non-Abelian gauge potential (43) generates such a mixing for non-zero values of the coupling g .

The choice of the gauge potentials is not unique. At any orientation (θ, ϕ) of the rotor's symmetry axis, the body-fixed coordinate system is defined up to an arbitrary rotation around the z' axis. Thus, the intrinsic degrees of freedom (of the fermion in our case) depend on a convention which is arbitrary. Different choices of the body-fixed system lead to different expressions for the covariant derivative and to different gauge potentials [53]. These are related to each other by gauge transformations. Details are given in Appendix E.

IV. LAGRANGIAN AND HAMILTONIAN

A. Leading-order terms

Collecting the leading-order results from the previous Sections, we find that the Lagrangian is given by

$$\begin{aligned} L &= \frac{C_0}{2} \mathbf{v}^2 + \mathbf{v} \cdot (\mathbf{A}_a + \mathbf{A}_n) + L_\Psi \\ &= \frac{C_0}{2} \left(\dot{\theta}^2 + \dot{\phi}^2 \sin^2 \theta \right) + g \left(\dot{\phi} \sin \theta \hat{K}_{x'} - \dot{\theta} \hat{K}_{y'} \right) \\ &\quad + \dot{\phi} \cos \theta \hat{K}_{z'} + L_\Psi . \end{aligned} \quad (47)$$

Here, L_Ψ is defined in Eq. (26). The Legendre transform of the Lagrangian (47) yields the Hamiltonian. For L_ψ that was done in Section II B. For the remaining variables the transformation is less tedious than might appear at first sight. The Lagrangian (47) is a quadratic form in the velocities $(\dot{\theta}, \dot{\phi})$ and can be written as

$$L = \frac{1}{2} \dot{\mathbf{q}}^T \hat{M} \dot{\mathbf{q}} + \mathbf{A} \cdot \dot{\mathbf{q}} , \quad (48)$$

where T denotes the transpose. That Lagrangian has the Legendre transform

$$H = \frac{1}{2} (\mathbf{q} - \mathbf{A})^T \hat{M}^{-1} (\mathbf{q} - \mathbf{A}) . \quad (49)$$

Here, \hat{M} is a ‘‘mass’’ matrix and \hat{M}^{-1} denotes its inverse. In the present case the canonical momenta are

$$\begin{aligned} p_\phi &\equiv \frac{\partial L}{\partial \dot{\phi}} = C_0 v_\phi \sin \theta + \cos \theta \hat{K}_{z'} + g \sin \theta \hat{K}_{x'} , \\ p_\theta &\equiv \frac{\partial L}{\partial \dot{\theta}} = C_0 v_\theta - g \hat{K}_{y'} . \end{aligned} \quad (50)$$

Here, we employed Eq. (10). The Hamiltonian becomes

$$\begin{aligned} H &= H_\psi + \frac{1}{2C_0} \left(p_\theta + g \hat{K}_{y'} \right)^2 \\ &\quad + \frac{1}{2C_0} \left(\frac{p_\phi}{\sin \theta} - \cot \theta \hat{K}_{z'} - g \hat{K}_{x'} \right)^2 . \end{aligned} \quad (51)$$

Here, the fermion Hamiltonian H_ψ is given in Eq. (28). The momentum p_ϕ is conserved because ϕ does not appear in the Hamiltonian (51). Combining two of the canonical momenta (50) into

$$\mathbf{p} = p_\theta \mathbf{e}_\theta + \frac{p_\phi}{\sin \theta} \mathbf{e}_\phi , \quad (52)$$

we find

$$\mathbf{p} = C_0 \mathbf{v} + \mathbf{A}_a + \mathbf{A}_n . \quad (53)$$

Using that, we write the Hamiltonian (51) in compact form as

$$H = H_\psi + \frac{1}{2C_0} (\mathbf{p} - \mathbf{A}_a - \mathbf{A}_n)^2 = H_\psi + \frac{1}{2} C_0 \mathbf{v}^2 . \quad (54)$$

B. Angular momentum

Replacing the canonical momenta by the total angular momentum simplifies the Hamiltonian and establishes the connection to Eq. (2). In the present Subsection we introduce the total angular momentum on an intuitive basis. A derivation based on Noether’s theorem is given in App. B 3.

The total angular momentum

$$\mathbf{I} = \mathbf{I}_\perp + \mathbf{I}_{z'} \quad (55)$$

is the sum of the angular momentum of the fermion,

$$\mathbf{I}_{z'} = \mathbf{e}'_z \hat{K}_{z'} , \quad (56)$$

which points in the direction of the symmetry axis, and that of the rotor,

$$\begin{aligned} \mathbf{I}_\perp &= I_{x'} \mathbf{e}'_x + I_{y'} \mathbf{e}'_y \\ &= p_\theta \mathbf{e}'_y - \left(\frac{p_\phi}{\sin \theta} - \cot \theta \hat{K}_{z'} \right) \mathbf{e}'_x \\ &= \mathbf{r} \times (\mathbf{p} - \mathbf{A}_a) . \end{aligned} \quad (57)$$

which is perpendicular to it. In the last line of Eq. (57) we have used Eq. (53), see also Refs. [68, 69]. The term $\mathbf{r} \times \mathbf{p}$ is the angular momentum $C_0 \mathbf{r} \times \mathbf{v}$ of the rotor. The gauge

potential \mathbf{A}_a is not manifestly invariant under rotations but can be made so via a gauge transformation [68]. That causes the correction (56) in the direction of \mathbf{e}'_z . The equality

$$I_z \equiv \mathbf{e}_z \cdot \mathbf{I} = p_\phi . \quad (58)$$

shows that the conserved momentum p_ϕ is the usual angular momentum with respect to the space-fixed z axis. We use Eqs. (57) and (55) to express the angular velocity in terms of the angular momentum. That yields

$$\mathbf{v} = -\frac{1}{C_0} (\mathbf{e}'_z \times \mathbf{I} + \mathbf{A}_n) . \quad (59)$$

Using that in the rotational energy $(C_0/2)\mathbf{v}^2$, we arrive at the Hamiltonian

$$\begin{aligned} H &= H_\Psi + \frac{g^2}{2C_0} \left(\hat{K}_{x'}^2 + \hat{K}_{y'}^2 \right) \\ &\quad + \frac{\mathbf{I}^2 - \hat{K}_{z'}^2}{2C_0} + \frac{g}{C_0} \left(I_{x'} \hat{K}_{x'} + I_{y'} \hat{K}_{y'} \right) . \end{aligned} \quad (60)$$

The term proportional to g^2 in Eq. (60) might be absorbed into H_Ψ (and then be dropped). The rotational part displayed in the second line of Eq. (60) corresponds to the rotor model (2) for the special case of axial symmetry, i.e. for $C_{x'} = C_{y'}$.

The square of the total angular momentum is given by

$$\begin{aligned} \mathbf{I}^2 &= p_\theta^2 + \frac{1}{\sin^2 \theta} \left(p_\phi - \cos \theta \hat{K}_{z'} \right)^2 + \hat{K}_{z'}^2 \\ &= p_\theta^2 + \frac{1}{\sin^2 \theta} \left(p_\phi^2 - 2p_\phi \cos \theta \hat{K}_{z'} + \hat{K}_{z'}^2 \right) . \end{aligned} \quad (61)$$

Upon quantization this operator, its projection $I_{z'} = \hat{K}_{z'}$ onto the z' -axis [see Eq. (56)], and its projection $I_z = p_\phi$ onto the z -axis [see Eq. (58)] form a commuting set of operators. Details are presented in Appendix B 3.

C. Spectrum

Simplifying the notation used in Eq. (32) we denote the ground state of the fermionic part of the Hamiltonian (60) as $|K\rangle$. We calculate the eigenfunctions of the rotor part of the Hamiltonian (60) by determining the eigenfunctions of \mathbf{I}^2 , I_z , and $I_{z'}$. For states $|\pm K\rangle$ we have

$$I_{z'} |\pm K\rangle = \hat{K}_{z'} |\pm K\rangle = \pm K |\pm K\rangle . \quad (62)$$

The quantization proceeds as in Section II. The eigenfunctions of $I_z = p_\phi = -i\partial_\phi$ are

$$I_z e^{-iM\phi} = -M e^{-iM\phi} . \quad (63)$$

The negative eigenvalue is chosen here to be consistent with chapter 4.2 of Ref. [52]. The eigenfunctions of the square of the total angular momentum operator can be written either in terms of Wigner d functions or in terms

of Wigner D functions (see chapter 4 of Ref. [52]). These are related by

$$D_{M,M'}^I(\phi, \theta, 0) = e^{-iM\phi} d_{M,M'}^I(\theta). \quad (64)$$

For $I \geq |M|, |K|$ we have

$$\mathbf{I}^2 D_{M,\mp K}^I(\phi, \theta, 0)|\pm K\rangle \quad (65)$$

$$= I(I+1) D_{M,\mp K}^I(\phi, \theta, 0)|\pm K\rangle. \quad (66)$$

For the Hamiltonian (60) that implies

$$\begin{aligned} & \frac{\mathbf{I}^2 - \hat{K}_{z'}^2}{2C_0} D_{M,\mp K}^I(\phi, \theta, 0)|\pm K\rangle \\ &= \frac{I(I+1) - K^2}{2C_0} D_{M,\mp K}^I(\phi, \theta, 0)|\pm K\rangle. \end{aligned} \quad (67)$$

Discrete symmetries of the rotor-plus-fermion system may select a definite linear combination of the states $|\pm K\rangle$. These share the absolute value $|K|$ and have the same energy $E_{|K|}$ [see Eq. (32)]. Combining $E_{|K|}$ with Eq. (67) yields

$$E(I) = E_{|K|} + \frac{I(I+1) - K^2}{2C_0}. \quad (68)$$

The term linear in g of the Hamiltonian (60) couples states $D_{M,-K}^I|K\rangle$ and $D_{M,-K\mp 1}^I|K\pm 1\rangle$. For most heavy nuclei where $\xi \ll \Omega$, the coupling of states with different values of $|K|$ is of subleading order and can be computed perturbatively. For $K = \pm 1/2$, however, the interaction couples the degenerate states $D_{M,\mp \frac{1}{2}}^I|\pm \frac{1}{2}\rangle$ and is, thus, of leading order ξ . For this case, eigenfunctions and eigenvalues are worked out in Appendix F. The result for the eigenvalues,

$$\begin{aligned} E(I, K) &= E_{|K|} + \frac{I(I+1) - K^2}{2C_0} \\ &\quad - \frac{g}{C_0} \delta_{|K|, \frac{1}{2}} (-1)^{I+\frac{1}{2}} \left(I + \frac{1}{2} \right), \end{aligned} \quad (69)$$

agrees with Eq. (22) when we express the constants $E_{|K|}$, C_0 , and g in terms of E_0 , A , and a . The last term in Eq. (69) is known as the signature splitting. Equation (69) shows that for $g \neq 0$ the spectrum changes by about $g\xi$. For $|g| \gg 1$, the spectrum would resemble a rotational band only for $I \gtrsim |g|$. This confirms that the natural size of g is of order unity.

States that differ by one unit in K can also be coupled strongly by the term linear in g in the Hamiltonian (60) provided $\Omega \approx \xi$. In that case, the spectrum can be calculated analytically using as a basis the eigenstates obtained for $g = 0$ and taking account only of the two bandheads. The diagonalization of the 4×4 matrix spanned by the states $|\pm K\rangle$ and $|\pm(K+1)\rangle$ yields the

eigenvalues [28]

$$\begin{aligned} E(I, K, K+1) &= \frac{1}{2} [E(I, K) + E(I, K+1)] \\ &\quad \pm \frac{1}{2} \left\{ [E(I, K) - E(I, K+1)]^2 \right. \\ &\quad \left. + 4 \frac{\tilde{g}^2}{C_0^2} [I(I+1) - K(K+1)] \right\}^{\frac{1}{2}}. \end{aligned} \quad (70)$$

The energies $E(I, K)$ are given by Eq. (69), and $\tilde{g} \equiv g\langle K|\hat{K}_{-1}|K+1\rangle$ is a low-energy constant. The sign on the right-hand side of Eq. (70) has to be chosen such that the energies $E(I, K)$ and $E(I, K+1)$ for the bands with quantum numbers K and $K+1$, respectively, are obtained as $g \rightarrow 0$. In nuclei such as $^{105,107}\text{Mo}$, groups of more than two band heads are closely spaced and strongly coupled. In such cases, a Hamiltonian matrix of larger dimension needs to be diagonalized.

We discuss our results. For $g = 0$, the total angular momentum \mathbf{I}^2 and its projections I_z and $I_{z'}$ onto the space- and body-fixed z -axes, respectively, commute with each other and with the Hamiltonian. The spectrum is given by Eq. (68). The nucleus is axially symmetric because $I_{z'}$ is conserved. For finite g , the projection of the angular momentum onto the rotor's symmetry axis is not conserved because the Abelian and non-Abelian gauge potentials do not commute. According to the rules for power counting, the term linear in g (the ‘‘Coriolis term’’) is of leading order. Nevertheless, the impact of the Coriolis term on the spectrum depends very much on the nucleus under consideration. In a band with band-head spin K this term contributes of the order $\xi(\xi/\Omega)^{K-1/2}$. Thus, it is only of leading order for a rotational band with $K = 1/2$. However, the Coriolis term also couples bands that differ in $|K|$ by one unit. Equation (70) shows that the Coriolis term is of leading order only if $\tilde{g} \equiv g\langle K|\hat{K}_{-1}|K+1\rangle$ is sufficiently large, i.e. of order unity. In practice, this is mostly expected if two band heads that differ in spin by one unit are closely spaced in energy. Here ‘‘close’’ means that the spacing is not of the typical fermion scale Ω but rather of the rotational scale ξ . In the presence of the Coriolis term, $I_{z'}$ is not a conserved quantity anymore, and the odd-mass nucleus exhibits triaxial deformation. We illustrate this behavior below for ^{187}Os . From the point of view of our EFT, triaxiality in odd-mass nuclei thus depends on the spins of band heads and on their separation in energy.

D. Next-to-leading order corrections

The leading-order Hamiltonian (60) contains contributions that scale as ξ and/or Ω . Out of the many terms quadratic in both \mathbf{v} and \mathbf{K} that one can write down using \mathbf{v} , \mathbf{K} , and \mathbf{e}'_z , the following combinations are linearly

independent and compatible with the symmetries:

$$\begin{aligned} L_{1a} &= \frac{g_a}{2} \mathbf{v}^2 (K_{x'}^2 + K_{y'}^2) , \\ L_{1b} &= \frac{g_b}{2} \mathbf{v}^2 K_{z'}^2 , \\ L_{1c} &= \frac{g_c}{2} (\mathbf{v} \cdot \mathbf{K})^2 . \end{aligned} \quad (71)$$

The natural assumption is that $g_{a,b,c} \sim \Lambda^{-1}$. Then, the contributions of $L_{1a,b,c}$ scale as ξ^2/Λ , which is a factor ξ/Λ smaller than the leading-order Lagrangian (47). The next-to-leading order terms (71) are still quadratic in the velocities. After adding these terms to the Lagrangian (47) we can, therefore, perform the Legendre transform as outlined in Subsection IV A, but invert the mass matrix perturbatively. The calculation is done in Appendix F. The resulting Hamiltonian is

$$H = H_{\text{LO}} + H_{\text{NLO}} , \quad (72)$$

with the leading-order Hamiltonian H_{LO} as in Eq. (60) and with

$$H_{\text{NLO}} = \frac{1}{2C_0} (\mathbf{N}^T \hat{C} \mathbf{N} + \mathbf{N}^T \hat{G} \mathbf{N}) . \quad (73)$$

The dimensionless operators \hat{C} and \hat{G} are all of order ξ/Λ and depend on bilinear combinations of the fermion operators $\hat{K}_{x'}$, $\hat{K}_{y'}$, and $\hat{K}_{z'}$. In Eq. (73) we also used

$$\mathbf{N} \equiv \begin{pmatrix} I_{y'} \\ I_{x'} \end{pmatrix} + g \begin{pmatrix} \hat{K}_{y'} \\ \hat{K}_{x'} \end{pmatrix} . \quad (74)$$

The matrix \hat{C} , due to $L_{1a,b}$, is diagonal in the eigenstates of the leading-order Hamiltonian (60). Thus, the first term on the right-hand side of Eq. (73) adds a fermion-state dependent correction of order ξ^2/Λ to the moment of inertia. It causes the moments of inertia of rotational bands in odd mass nuclei to deviate somewhat from the moment of inertia for the ground-state band of the even-even rotor. The correction can be compared to the smaller variations of order (ξ^3/Λ^2) that occur in even-even nuclei [70]. The matrix \hat{G} (due to L_{1c}) in the second term is traceless and mixes fermion states that differ in quantum numbers $K_{z'}$ by two units. In particular, this term modifies the rotational spectra of $|K_{z'}| = 3/2$ band heads.

How does our approach compare with a treatment that would use full-fledged quantum field theory? While in the derivation of the EFT we employed velocities and canonical momenta, the solution of the Hamiltonian became simple because we introduced angular momenta. In the gauge we used the eigenfunctions are the Wigner D functions (64). These can be written as infinite sums of spherical harmonics, i.e. of the “free” solutions of the even-even rotor. We are convinced that using $\nabla_\Omega \rightarrow \nabla_\Omega - i\mathbf{A}_{\text{tot}}$, gauging the quantum-field theory Lagrangian (19 with the gauge potential (45), and using field-theoretical tools such as Feynman diagrams, would yield the same result. Then, the “free” rotor would scatter via infinite loops with the fermion, with vertices due to the gauge coupling.

V. APPLICATIONS

In the previous Section we have shown that in leading order, the EFT for odd-mass deformed nuclei recovers the results of the (axially symmetric) particle-rotor model. While that model is well known, with numerous applications to be found in textbooks [22, 23, 29, 31, 64] and in the literature, the EFT provides us, in addition, with a systematic approach to subleading corrections and to estimates of the uncertainty of EFT predictions [11]. We illustrate that point, following arguments made previously for even-even deformed nuclei with axial symmetry [44] and for vibrational excitations in heavy nuclei [19, 20].

A. ^{239}Pu

Within the EFT the nucleus ^{239}Pu is described as a neutron attached to ^{238}Pu . Inspection of the low-lying states of ^{238}Pu in Fig. 1 shows that the low-energy scale is $\xi \approx 44$ keV and the breakdown scale is $\Lambda \approx 600$ keV. This is probably too conservative an estimate for the breakdown scale of the ground-state band in ^{238}Pu , because the lowest band head with positive parity occurs at 941 keV. Thus, for a description of the ground-state band, $\xi/\Lambda \approx 1/21$ is probably a more accurate estimate for the expansion parameter. Adjusting the low-energy constant C_0 to the energy of the 2^+ state yields $1/(2C_0) = 7.35$ keV. The leading-order EFT predictions [12, 44] for the ground-state rotational band are levels at energies

$$E_{\text{LO}}(I) = \frac{I(I+1)}{2C_0} \left[1 + \mathcal{O} \left(\frac{\xi^2}{\Lambda^2} \right) I(I+1) \right] . \quad (75)$$

Here, we included the EFT uncertainty estimate [12, 44]. Figure 3 compares the EFT results to data. For the uncertainty estimate we used $\mathcal{O} \left(\frac{\xi^2}{\Lambda^2} \right) = 0.25(\xi/\Lambda)^2$, where the factor 0.25 is determined empirically.

In leading order, the rotational constant of the nucleus ^{239}Pu is the same as for ^{238}Pu . We only have to adjust the constant g in Eq. (69) to describe the ground-state band. A fit to the first excited state in this nucleus yields $g = -0.642$. The resulting ground-state band is shown in the left part of Fig. 4 and compared to data in the center. At leading order, the rotational constant has a relative uncertainty of $\mathcal{O}(\xi/\Lambda)$, as reflected by the blue shaded areas. For the displayed uncertainties, we used the conservative estimate $\xi/\Lambda = 1/14$ and $\mathcal{O}(\xi/\Lambda) = 2\xi/\Lambda$, with the factor of 2 determined empirically.

A next-to-leading order fit to the energies $E(I, 1/2)$ of Eq. (69) is shown in the right part of Fig. 4. Here, we adjusted both C_0 and g in Eq. (69), finding $1/(2C_0) = 6.257$ keV and $g = -0.579$. We note that the change of C_0 by about a factor of $2\xi/\Lambda$ is consistent with EFT expectations. At next-to-leading order, relative energy uncertainties are estimated as $2C_0 E(I, 1/2) \mathcal{O}(\xi^2/\Lambda^2)$ with

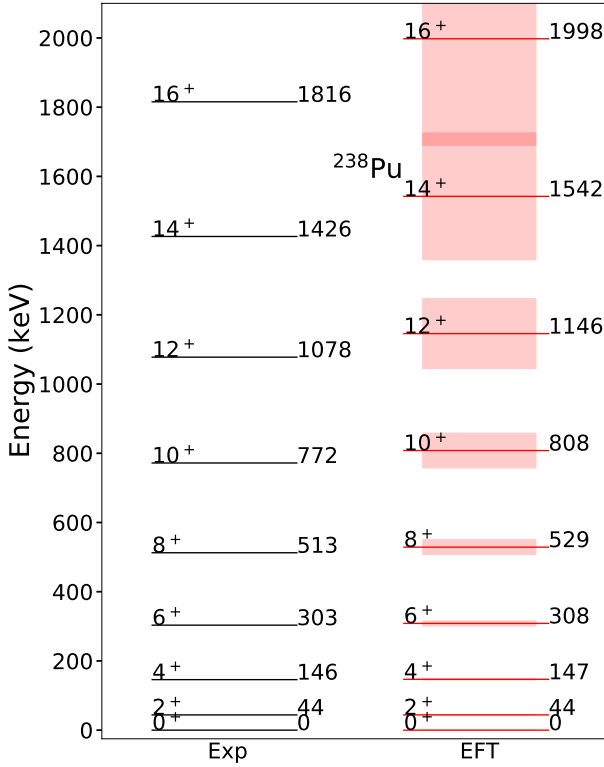


FIG. 3. (Color online) Levels of the ground-state rotational band in ^{238}Pu , with spin/parity and energy as indicated, from data (left, black) are compared to EFT predictions (red, right) at leading order [$\mathcal{O}(\xi)$] with uncertainty estimates (shaded red areas).

$\mathcal{O}(\xi^2/\Lambda^2) = (0.25\xi/\Lambda)^2$. As before, the factor 0.25 is determined empirically.

We see that the EFT yields an accurate (it agrees with the data within the uncertainties) and increasingly precise (as more orders are included) description of the ground-state rotational band of ^{239}Pu . Furthermore, the low-energy constants are not merely fit parameters, but the size of subleading corrections can be estimated from the empirical values of the low-energy scale ξ and the breakdown scale Λ . Similar results can also be obtained for the other rotational bands displayed in Fig. 2.

B. ^{187}Os

In most odd-mass nuclei, the Coriolis term [last term in Eq. (60)] that couples different rotational bands enters only perturbatively, because band heads that differ in K by one unit are usually an energy $\Omega \gg \xi$ apart. However, in nuclei with closely spaced band heads, the Coriolis term is of leading order. Among these are the light nucleus ^9Be , the nuclei ^{49}Cr and ^{49}Mn , $^{105,107}\text{Mo}$, ^{187}Ir , and ^{187}Os . We illustrate our results for the well-studied nucleus ^{187}Os [71–73]. The $K^\pi = 1/2^-$ ground state exhibits a rotational band with a low-energy con-

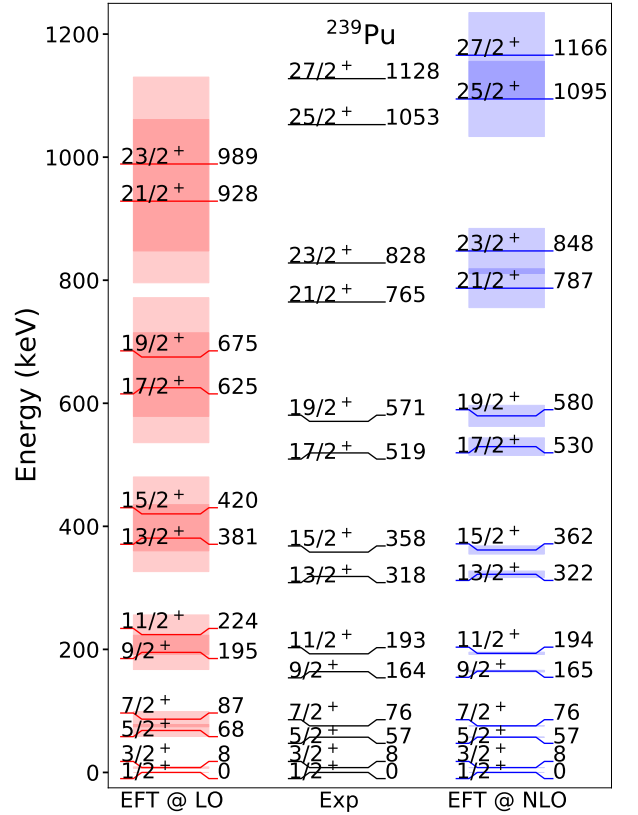


FIG. 4. (Color online) Levels of the ground-state rotational band in ^{239}Pu , with spin/parity and energy as indicated, from data (center, black) are compared to EFT predictions at leading order (red, left) and at next-to-leading order (blue, right) with uncertainty estimates (shaded areas).

stant $C_0^{-1} \approx 47$ keV. The first excited $K^\pi = 3/2^-$ band head is only separated by $\Omega \approx 10$ keV. Thus, we have $\xi \sim \Omega$, the two bands in question are coupled by the Coriolis term, and Eqs. (70) must be employed.

The relevant scales are as follows. The even-even nucleus ^{186}Os exhibits a ground-state rotational band with a 2^+ state at 137 keV; the excited 2^+ band head at 770 keV sets the breakdown scale Λ of this rotor. The ratio of the energies of the two lowest 2^+ states is $\xi/\Lambda \approx 1/6$. In a first step we neglect the coupling between the $K^\pi = 1/2^-$ and $K^\pi = 3/2^-$ bands in ^{187}Os . Adjusting a total of five parameters [C_0 , $E_{1/2}$, and g in Eq. (69)] to the lowest three states for $K^\pi = 1/2^-$ and fitting separately C_0 and $E_{3/2}$ to the two states of the $K^\pi = 3/2^-$ band yields the two rotational bands shown in left part of Fig. 5. Here, the highest two (three) states of the $K^\pi = 1/2^-$ ($K^\pi = 3/2^-$) band, respectively, are predictions. The results are to be compared to the data shown in the center. Also shown in the right part are the EFT predictions obtained by adjusting the five parameters C_0 , $E_{1/2}$, $E_{3/2}$, g , and \tilde{g} in Eq. (70) simultaneously to the lowest three states of both bands. Given the same number (five) of low-energy constants, the improved ac-

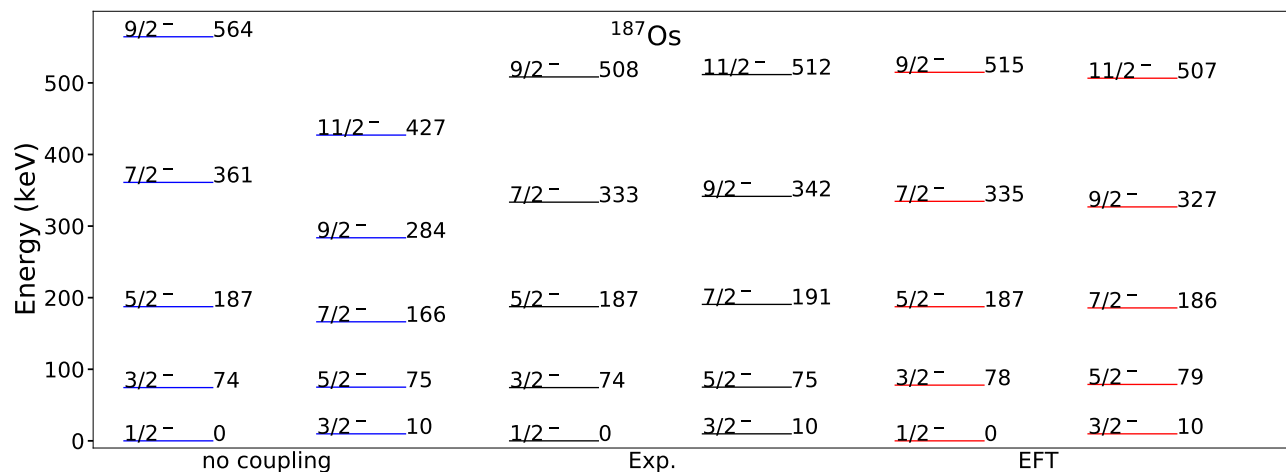


FIG. 5. (Color online) Levels of the two lowest-lying rotational bands in ^{187}Os , with spin/parity and energy as indicated. Center (black): Data. Left (blue): Results obtained by fitting energies of both bands but neglecting the Coriolis coupling. Right (red): EFT fits with predictions at leading plus next-to-leading order. The relative EFT uncertainties (not shown) are about $2\xi^2/\Lambda^2 \approx 7\%$.

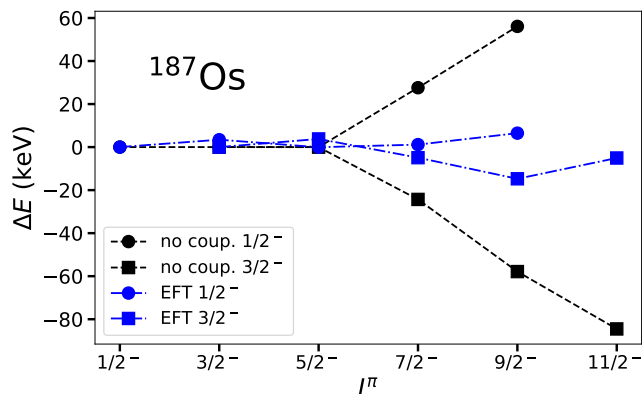


FIG. 6. (Color online) Energy differences between theory and data for the two lowest-lying rotational bands in ^{187}Os as a function of spin/parity. Results obtained by fitting energies of both bands but neglecting the Coriolis coupling are shown in black, and EFT results in blue. Circles and squares mark the rotational states on top of the $I^\pi = 1/2^-$ and $3/2^-$ band heads, respectively.

curacy obtained in the second fit shows the need to include the Coriolis coupling. Comparing the results to the data we infer that relative EFT uncertainties are about $2\xi^2/\Lambda^2 \approx 7\%$. Figure 6 shows the energy differences between theory and data for both bands using EFT (blue) and neglecting the coupling between the bands (black). We see that approach that neglects the coupling between the bands loses accuracy as soon as one considers states that were not fitted.

VI. SUMMARY

We have developed an effective field theory for deformed odd-mass nuclei. In this approach, the odd nucleon experiences an axially-symmetric potential in the body-fixed frame of the even-even deformed nucleus (a rotor). The power counting is based on the separation of scales between low-lying rotational degrees of freedom on the one hand and both, higher-lying nucleonic excitations and intrinsic excitations of the even-even nucleus, on the other. In leading order, the nucleon is coupled to the rotor via gauge potentials. Actually, the non-Abelian gauge potential is a truly first-order term only for $K = 1/2$ band heads or when band heads with K quantum numbers that differ by one unit of angular momentum, are close in energy. In the latter case, the gauge potential induces triaxiality. That was shown by applying the EFT to ^{187}Os . We have shown how subleading contributions can be constructed systematically, and how these may be used to improve the spectrum and/or to estimate theoretical uncertainties. The EFT developed in this paper presents a model-independent approach to the particle-rotor system that is capable of systematic improvement.

ACKNOWLEDGMENTS

This work has been supported by the U.S. Department of Energy under grant No. DE-FG02-96ER40963 and under contract DE-AC05-00OR22725 with UT-Battelle, LLC (Oak Ridge National Laboratory).

Appendix A: Overview

Appendix B presents details regarding transformation properties under rotations. In App. C we derive the expression for the covariant derivative. Appendix D presents a more formal derivation of these properties based on the coset approach. In App. E we discuss gauge potentials and gauge transformations. App. F presents details regarding the derivation of the spectrum and sub-leading corrections.

Appendix B: Transformation properties under rotations

In this Appendix we use infinitesimal rotations and apply Noether's theorem to derive the expressions in Section IV for the total angular momentum, both in the space-fixed and in the body-fixed system.

An infinitesimal rotation changes the angles (θ, ϕ) to $(\theta + \delta\theta, \phi + \delta\phi)$. That moves the symmetry axis of the rotor into a new direction, and it induces a rotation of the axes \mathbf{e}'_x and \mathbf{e}'_y around the rotors new symmetry axis by an angle $\delta\omega$. In the following two subsections, we relate the infinitesimal angles $(\delta\theta, \delta\phi, \delta\omega)$ to the parameters of a general infinitesimal rotation. We do so for rotations around the axes of the space-fixed system and for rotations around the body-fixed axes. We use that at the point $(\theta + \delta\theta, \phi + \delta\phi)$, the body-fixed basis vectors are

$$\begin{aligned} \mathbf{e}'_x(\phi + \delta\phi, \theta + \delta\theta) &= \mathbf{e}'_x(\phi, \theta) - \delta\theta \mathbf{e}'_z(\phi, \theta) \\ &\quad + \delta\phi \cos \theta \mathbf{e}'_y(\phi, \theta), \\ \mathbf{e}'_y(\phi + \delta\phi, \theta + \delta\theta) &= \mathbf{e}'_y(\phi, \theta) - \delta\phi \sin \theta \mathbf{e}'_z(\phi, \theta) \\ &\quad - \delta\theta \cos \theta \mathbf{e}'_x(\phi, \theta), \\ \mathbf{e}'_z(\phi + \delta\phi, \theta + \delta\theta) &= \mathbf{e}'_z(\phi, \theta) + \delta\theta \mathbf{e}'_x(\phi, \theta) \\ &\quad + \delta\phi \sin \theta \mathbf{e}'_y(\phi, \theta). \end{aligned} \quad (\text{B1})$$

1. Rotations around the space-fixed axes

A rotation by the vector $\delta\boldsymbol{\alpha} = \delta\alpha_x \mathbf{e}_x + \delta\alpha_y \mathbf{e}_y + \delta\alpha_z \mathbf{e}_z$ about infinitesimal angles $\delta\alpha_k$, $k = x, y, z$ around the space-fixed axes changes the body-fixed basis vectors \mathbf{e}'_k , $k = x, y, z$ by

$$\begin{aligned} \delta\boldsymbol{\alpha} \times \mathbf{e}'_x &= (\delta\boldsymbol{\alpha} \cdot \mathbf{e}'_z) \mathbf{e}'_y - (\delta\boldsymbol{\alpha} \cdot \mathbf{e}'_y) \mathbf{e}'_z, \\ \delta\boldsymbol{\alpha} \times \mathbf{e}'_y &= (\delta\boldsymbol{\alpha} \cdot \mathbf{e}'_x) \mathbf{e}'_z - (\delta\boldsymbol{\alpha} \cdot \mathbf{e}'_z) \mathbf{e}'_x, \\ \delta\boldsymbol{\alpha} \times \mathbf{e}'_z &= (\delta\boldsymbol{\alpha} \cdot \mathbf{e}'_y) \mathbf{e}'_x - (\delta\boldsymbol{\alpha} \cdot \mathbf{e}'_x) \mathbf{e}'_y. \end{aligned} \quad (\text{B2})$$

We equate the incremental changes of $\mathbf{e}'_z(\phi + \delta\phi, \theta + \delta\theta)$ on the right-hand side of the last of Eqs. (B1) with the last line of Eq. (B2). That yields

$$\begin{pmatrix} \delta\theta \\ \delta\phi \end{pmatrix} = \begin{bmatrix} -\sin \phi & \cos \phi & 0 \\ -\cos \phi \cot \theta & -\sin \phi \cot \theta & 1 \end{bmatrix} \begin{pmatrix} \delta\alpha_x \\ \delta\alpha_y \\ \delta\alpha_z \end{pmatrix}. \quad (\text{B3})$$

The rotor's degrees of freedom clearly transform nonlinearly, i.e., under the rotation by $\delta\boldsymbol{\alpha}$ they depend in a nonlinear way on (ϕ, θ) . The rotated basis vector $\mathbf{e}'_x + \delta\boldsymbol{\alpha} \times \mathbf{e}'_x$ differs from the basis vector $\mathbf{e}'_x(\phi + \delta\phi, \theta + \delta\theta)$ by a small rotation with the angle $\delta\omega$ around the rotor's symmetry axis $\mathbf{e}'_z(\phi + \delta\phi, \theta + \delta\theta)$. To determine $\delta\omega$ we compute the scalar product

$$\begin{aligned} \delta\omega &= [\mathbf{e}'_x(\phi, \theta) + \delta\boldsymbol{\alpha} \times \mathbf{e}'_x(\phi, \theta)] \cdot \mathbf{e}'_y(\phi + \delta\phi, \theta + \delta\theta) \\ &= \frac{\cos \phi}{\sin \theta} \delta\alpha_x + \frac{\sin \phi}{\sin \theta} \delta\alpha_y. \end{aligned} \quad (\text{B4})$$

The rotation by the infinitesimal angle $\delta\omega$ around the body-fixed z' -axis is induced by the operator $e^{-i\delta\omega J_{z'}}$. Under that transformation the spinor function $\hat{\Psi}(\mathbf{x}')$, defined in Eq. (25) in the body-fixed system, transforms as

$$\hat{\Psi}(\mathbf{x}') \rightarrow \hat{\Psi}(\mathbf{x}') + \delta\hat{\Psi}(\mathbf{x}') \quad (\text{B5})$$

where

$$\delta\hat{\Psi}(\mathbf{x}') = -i\delta\omega [J_{z'}, \hat{\Psi}(\mathbf{x}')] . \quad (\text{B6})$$

Collecting results from Eqs. (B3), (B4), and (B6) we find

$$\begin{pmatrix} \delta\theta \\ \delta\phi \\ \delta\hat{\Psi}(\mathbf{x}') \end{pmatrix} = \hat{T}_S \begin{pmatrix} \delta\alpha_x \\ \delta\alpha_y \\ \delta\alpha_z \end{pmatrix}, \quad (\text{B7})$$

where

$$\hat{T}_S \equiv \begin{bmatrix} -\sin \phi & \cos \phi & 0 \\ -\cos \phi \cot \theta & -\sin \phi \cot \theta & 1 \\ -i \frac{\cos \phi}{\sin \theta} [J_{z'}, \hat{\Psi}(\mathbf{x}')] & -i \frac{\sin \phi}{\sin \theta} [J_{z'}, \hat{\Psi}(\mathbf{x}')] & 0 \end{bmatrix}. \quad (\text{B8})$$

2. Rotation around the body-fixed axes

A rotation by the vector $\delta\boldsymbol{\alpha}' = \delta\alpha_{x'} \mathbf{e}'_x + \delta\alpha_{y'} \mathbf{e}'_y + \delta\alpha_{z'} \mathbf{e}'_z$ about infinitesimal angles $\delta\alpha_{k'}$, $k' = x', y', z'$ around the body-fixed axes changes the body-fixed basis vectors $\mathbf{e}'_{k'}$ by

$$\begin{aligned} \delta\boldsymbol{\alpha}' \times \mathbf{e}'_x &= \delta\alpha_{z'} \mathbf{e}'_y - \delta\alpha_{y'} \mathbf{e}'_z, \\ \delta\boldsymbol{\alpha}' \times \mathbf{e}'_y &= \delta\alpha_{x'} \mathbf{e}'_z - \delta\alpha_{z'} \mathbf{e}'_x, \\ \delta\boldsymbol{\alpha}' \times \mathbf{e}'_z &= \delta\alpha_{y'} \mathbf{e}'_x - \delta\alpha_{x'} \mathbf{e}'_y. \end{aligned} \quad (\text{B9})$$

Equating the incremental change of $\mathbf{e}'_z(\phi + \delta\phi, \theta + \delta\theta)$ on the right-hand side of the last of Eqs. (B1) with the last line of Eq. (B9) gives

$$\begin{pmatrix} \delta\theta \\ \delta\phi \end{pmatrix} = \begin{bmatrix} 0 & 1 & 0 \\ -\frac{1}{\sin \theta} & 0 & 0 \end{bmatrix} \begin{pmatrix} \delta\alpha_{x'} \\ \delta\alpha_{y'} \\ \delta\alpha_{z'} \end{pmatrix}. \quad (\text{B10})$$

The incremental rotation angle $\delta\omega'$ is given by the scalar product of the rotated basis vector $\mathbf{e}'_x + \delta\boldsymbol{\alpha}' \times \mathbf{e}'_x$ and the basis vector $\mathbf{e}'_y(\theta + \delta\theta, \phi + \delta\phi)$,

$$\begin{aligned} \delta\omega' &= [\mathbf{e}'_x(\theta, \phi) + \delta\boldsymbol{\alpha}' \times \mathbf{e}'_x(\theta, \phi)] \cdot \mathbf{e}'_y(\theta + \delta\theta, \phi + \delta\phi) \\ &= \delta\alpha_{x'} \cot \theta + \delta\alpha_{z'}. \end{aligned} \quad (\text{B11})$$

That shows that a rotation by $\delta\alpha'$ points the body-fixed system into the new direction $(\theta + \delta\theta, \phi + \delta\phi)$ and rotates the body fixed system around its new axis $\mathbf{e}'_z(\theta + \delta\theta, \phi + \delta\phi)$ by the angle $\delta\omega'$. The fermion wave function transforms as in Eqs. (B5, B6) but with $\delta\omega$ replaced by $\delta\omega'$. Thus,

$$\begin{pmatrix} \delta\theta \\ \delta\phi \\ \delta\hat{\Psi}(\mathbf{x}') \end{pmatrix} = \hat{T}_B \begin{pmatrix} \delta\alpha_{x'} \\ \delta\alpha_{y'} \\ \delta\alpha_{z'} \end{pmatrix}, \quad (\text{B12})$$

with

$$\hat{T}_B \equiv \begin{bmatrix} 0 & 1 & 0 \\ -\frac{1}{\sin\theta} & 0 & 0 \\ -i \cot\theta \left[J_{z'}, \hat{\Psi}(\mathbf{x}') \right] & 0 & -i \left[J_{z'}, \hat{\Psi}(\mathbf{x}') \right] \end{bmatrix}. \quad (\text{B13})$$

3. Noether's theorem and angular momentum

We use Noether's theorem [74] and the results of Subsections B1 and B2 to obtain expressions for the conserved quantities, i.e., the components of total angular momentum in the space-fixed and in the body-fixed system, respectively. These are used in Section IV of the main text.

The theorem expresses invariants of the system in terms of partial derivatives of the Lagrangian with respect to the velocities \dot{q}_ν of the system. The Lagrangian is given by the second of Eqs. (47), with L_Ψ defined in Eq. (26). The velocities are $\dot{\theta} \equiv \dot{q}_1$, $\dot{\phi} \equiv \dot{q}_2$, and the time derivative $\partial_t \hat{\Psi}(\mathbf{x}') \equiv \dot{q}(\mathbf{x}')$ of the fermion wave function. The conserved quantities are the components of angular momentum, expressed in terms of the transformation matrices of Eqs. (B8) and (B13) and given by

$$I_k = \sum_\nu \frac{\partial L}{\partial \dot{q}_\nu} \left[\hat{T}_S \right]_{\nu k} \quad (\text{B14})$$

for rotations around the space-fixed axes and

$$I_{k'} = \sum_\nu \frac{\partial L}{\partial \dot{q}_\nu} \left[\hat{T}_B \right]_{\nu k'} \quad (\text{B15})$$

for rotations around the body-fixed axes. In the case of the velocity $\dot{q}(\mathbf{x}')$, the summations on the right-hand sides of Eqs. (B14) and (B15) actually involve an integration over \mathbf{x}' . We use Eq. (50), perform the space integration over the matrix elements of $\hat{T}_{S,B}$, and use Eq. (31). In the space-fixed system we find

$$\begin{aligned} I_x &= -\sin\phi p_\theta - \cos\phi \cot\theta p_\phi + \hat{K}_{z'} \frac{\cos\phi}{\sin\theta}, \\ I_y &= \cos\phi p_\theta - \sin\phi \cot\theta p_\phi + \hat{K}_{z'} \frac{\sin\phi}{\sin\theta}, \\ I_z &= p_\phi. \end{aligned} \quad (\text{B16})$$

In the body-fixed system we have

$$\begin{aligned} I_{x'} &= -\frac{p_\phi - \hat{K}_{z'} \cos\theta}{\sin\theta}, \\ I_{y'} &= p_\theta, \\ I_{z'} &= \hat{K}_{z'}. \end{aligned} \quad (\text{B17})$$

The square of the total angular momentum, defined by the sum of the squares of its components and calculated either in the space-fixed or in the body-fixed system, in both cases is given by Eq. (61). Upon quantization, the components (B17) do not fulfill the canonical commutation relations as they are not generators of rotations. For a discussion of unusual commutation relations we refer the reader to Ref. [75].

Appendix C: Covariant derivative

For the time derivative of a vector $\mathbf{a} = a_{x'}\mathbf{e}'_x + a_{y'}\mathbf{e}'_y$ in the tangential plane of the two-sphere at \mathbf{e}'_z , we use

$$\begin{aligned} \dot{\mathbf{e}}_{x'} &= -\dot{\theta}\mathbf{e}'_z + \dot{\phi}\cos\theta\mathbf{e}'_y, \\ \dot{\mathbf{e}}_{y'} &= -\dot{\phi}\sin\theta\mathbf{e}'_z - \dot{\theta}\cos\theta\mathbf{e}'_x, \end{aligned} \quad (\text{C1})$$

and have

$$\begin{aligned} \dot{\mathbf{a}} &= (\dot{a}_{x'} - a_{y'}\dot{\phi}\cos\theta)\mathbf{e}'_x + (\dot{a}_{y'} + a_{x'}\dot{\phi}\cos\theta)\mathbf{e}'_y \\ &\quad - (a_{x'}\dot{\theta} + a_{y'}\dot{\phi}\sin\theta)\mathbf{e}'_z. \end{aligned} \quad (\text{C2})$$

The projection of $\dot{\mathbf{a}}$ onto the tangential plane defines the covariant derivative

$$\begin{aligned} D_t \mathbf{a} &\equiv (\dot{a}_{x'} - a_{y'}\dot{\phi}\cos\theta)\mathbf{e}'_x + (\dot{a}_{y'} + a_{x'}\dot{\phi}\cos\theta)\mathbf{e}'_y \\ &= \partial_t \mathbf{a} - i\dot{\phi}\cos\theta J_{z'} \mathbf{a}. \end{aligned} \quad (\text{C3})$$

The covariant derivative consists of the usual time derivative and a rotation in the tangential plane, i.e., a rotation by $\dot{\phi}\cos\theta$ around the \mathbf{e}'_z axis.

It is straightforward to generalize this argument to spin functions. Let χ_{Sm} with spin S and projection m be the spin function in the space-fixed system. A rotation to the body-fixed system yields the helicity spin states

$$\chi_{S\lambda}(\theta, \phi) = \sum_m D_{m\lambda}^S(\phi, \theta, 0) \chi_{Sm}. \quad (\text{C4})$$

These are quantized with respect to the body-fixed z' axis, see chapter 6.1.3 of Ref. [52]. The time derivative is

$$\begin{aligned} \dot{\chi}_{S\lambda}(\theta, \phi) &= \frac{\dot{\theta}}{2} \sqrt{S(S+1) - \lambda(\lambda-1)} \chi_{S\lambda-1}(\theta, \phi) \\ &\quad - \frac{\dot{\phi}}{2} \sqrt{S(S+1) - \lambda(\lambda+1)} \chi_{S\lambda+1}(\theta, \phi) \\ &\quad - i\dot{\phi} \sum_m m D_{m\lambda}^S(\phi, \theta, 0) \chi_{Sm}. \end{aligned} \quad (\text{C5})$$

Here we used formulas from chapter 4.9 of Ref. [52]. We also find

$$\begin{aligned} mD_{m\lambda}^S(\phi, \theta, 0) &= \lambda \cos \theta D_{m\lambda}^S(\phi, \theta, 0) \\ &- \frac{\sin \theta}{2} \sqrt{S(S+1) - \lambda(\lambda-1)} D_{m\lambda-1}^S(\phi, \theta, 0) \\ &- \frac{\sin \theta}{2} \sqrt{S(S+1) - \lambda(\lambda+1)} D_{m\lambda+1}^S(\phi, \theta, 0). \end{aligned} \quad (\text{C6})$$

This allows us to perform the sum, and we arrive at

$$\begin{aligned} \dot{\chi}_{S\lambda}(\theta, \phi) &= -i\dot{\phi} \cos \theta [J_{z'}, \chi_{S\lambda}(\theta, \phi)] \\ &+ \frac{1}{2} (v_\theta + iv_\phi) \sqrt{S(S+1) - \lambda(\lambda-1)} \chi_{S\lambda-1}(\theta, \phi) \\ &- \frac{1}{2} (v_\theta - iv_\phi) \sqrt{S(S+1) - \lambda(\lambda+1)} \chi_{S\lambda+1}(\theta, \phi). \end{aligned} \quad (\text{C7})$$

Here, we used $[J_{z'}, \chi_{S\lambda}(\theta, \phi)] = \lambda \chi_{S\lambda}(\theta, \phi)$. To obtain the part relevant for the covariant derivative we project the right-hand side of Eq. (C7) back onto $\chi_{S\lambda}(\theta, \phi)$. For a general spin function $\eta(t) = \sum_\lambda \eta^\lambda(t) \chi_{S\lambda}(\theta, \phi)$ in the body-fixed system we thus have

$$D_t \eta = \partial_t \eta - i\dot{\phi} \cos \theta [J_{z'}, \eta]. \quad (\text{C8})$$

Had we written the vector \mathbf{a} considered above in terms of its spherical components we would have obtained the same result. Applying the result (C8) to the spinor functions $\hat{\Psi}(\mathbf{x}')$ yields Eq. (38).

Appendix D: Coset space

We exploit the nonlinear realization of rotational invariance more formally than done in the calculations of Apps. B and C. Thereby we connect to previous EFTs on axially deformed nuclei [12, 13, 44], nuclei with triaxial deformation [16–18], and magnets [54–57]. We follow closely the original papers [46–48]. For reviews of this approach, and an exhibition for non-relativistic systems, we refer the readers to Refs. [49, 51, 76] and the textbook [77]. In finite systems, one speaks of emergent symmetry breaking [45] but the tools from field theory can also be extended to this case [12, 13, 78]. Not surprisingly, the calculations in the present Section have much in common with those in Appendices B1 and B2.

Three mutually orthogonal unit vectors ($|\mathbf{e}'_x\rangle, |\mathbf{e}'_y\rangle, |\mathbf{e}'_z\rangle$) (the “body-fixed system”) are linked to another three mutually orthogonal unit vectors ($|\mathbf{e}_x\rangle, |\mathbf{e}_y\rangle, |\mathbf{e}_z\rangle$) (the “space-fixed system”) by a rotation g so that for $k = x, y, z$ we have $|\mathbf{e}'_k\rangle = g|\mathbf{e}_k\rangle$. That can be written as $|\mathbf{e}'_k\rangle = \sum_j |\mathbf{e}_j\rangle \langle \mathbf{e}_j | g | \mathbf{e}_k \rangle = \sum_j |\mathbf{e}_j\rangle g_{jk}$ where $g_{jk} = \langle \mathbf{e}_j | g | \mathbf{e}_k \rangle$ is the matrix representation of g . The matrix g_{jk} is real orthogonal, $g_{jk} = (g^{-1})_{kj}$, hence $|\mathbf{e}_j\rangle = \sum_k g_{jk} |\mathbf{e}'_k\rangle$. Altogether,

$$|\mathbf{e}_j\rangle = \sum_k g_{jk} |\mathbf{e}'_k\rangle, \quad |\mathbf{e}'_k\rangle = \sum_j (g^{-1})_{kj} |\mathbf{e}_j\rangle. \quad (\text{D1})$$

For vectors we use small (capital) letters when they are written in the space-fixed (the body-fixed) system, respectively. For a vector $\mathbf{a} = \sum_j a_j |\mathbf{e}_j\rangle$ we have $\mathbf{A} = \sum_j A_j |\mathbf{e}'_j\rangle$ where

$$A_j = \sum_k (g^{-1})_{jk} a_k. \quad (\text{D2})$$

The transformation g is defined as

$$g(\theta, \phi) = \exp\{-i\phi J_z\} \exp\{-i\theta J_y\}. \quad (\text{D3})$$

It coincides with the transformation $\mathcal{R}(\phi, \theta, 0)$ in Section II A. The three generators J_k of infinitesimal rotations about the k -axes obey

$$[J_x, J_y] = iJ_z \text{ (cyclic)}. \quad (\text{D4})$$

The matrix representation of the operators J_x, J_y, J_z is

$$\begin{aligned} -iJ_x &\rightarrow \begin{pmatrix} 0 & 0 & 0 \\ 0 & 0 & -1 \\ 0 & 1 & 0 \end{pmatrix}, \\ -iJ_y &\rightarrow \begin{pmatrix} 0 & 0 & 1 \\ 0 & 0 & 0 \\ -1 & 0 & 0 \end{pmatrix}, \\ -iJ_z &\rightarrow \begin{pmatrix} 0 & -1 & 0 \\ 1 & 0 & 0 \\ 0 & 0 & 0 \end{pmatrix}. \end{aligned} \quad (\text{D5})$$

The commutation relations (D4) for the matrix representation are verified using standard matrix algebra. The relations (D5) imply

$$\begin{aligned} \exp\{-i\phi J_z\} &\rightarrow \begin{pmatrix} \cos \phi & -\sin \phi & 0 \\ \sin \phi & \cos \phi & 0 \\ 0 & 0 & 1 \end{pmatrix}, \\ \exp\{-i\theta J_y\} &\rightarrow \begin{pmatrix} \cos \theta & 0 & \sin \theta \\ 0 & 1 & 0 \\ -\sin \theta & 0 & \cos \theta \end{pmatrix}, \end{aligned} \quad (\text{D6})$$

and, thus,

$$g \rightarrow \begin{pmatrix} \cos \phi \cos \theta & -\sin \phi \cos \phi \sin \theta \\ \sin \phi \cos \theta & \cos \phi \sin \phi \sin \theta \\ -\sin \theta & 0 & \cos \theta \end{pmatrix}. \quad (\text{D7})$$

In the body-fixed system, we define a set of three operators \tilde{J}_k , $k = x, y, z$. These have the same commutation relations (D4) as the operators J_k . Moreover, these operators have, by definition, the same matrix representation (D5) in the basis $|\mathbf{e}'_k\rangle$ as do the operators J_k in the basis $|\mathbf{e}_k\rangle$. Hence, with

$$g = \sum_\mu |\mathbf{e}'_\mu\rangle \langle \mathbf{e}_\mu|, \quad g^{-1} = \sum_\mu |\mathbf{e}_\mu\rangle \langle \mathbf{e}'_\mu| \quad (\text{D8})$$

we have for $k = x, y, z$

$$\tilde{J}_k = g J_k g^{-1}, \quad J_k = g^{-1} \tilde{J}_k g. \quad (\text{D9})$$

The commutation relations for the operators \tilde{J}_k differ in sign from the anomalous commutators commonly used in the body-fixed system. The reason is that the definition (D9) employs the matrix representation of J_k on its right-hand side. Conventionally, when using differential operators for J_k , these act also on the angles in g and one obtains additional transformation terms leading to anomalous commutation relations. The operators J_k and \tilde{J}_k differ. That is seen by comparing the matrix representations in the basis $|\mathbf{e}_l\rangle$,

$$\langle \mathbf{e}_l | \tilde{J}_k | \mathbf{e}_m \rangle = \sum_{nr} g_{ln} \langle \mathbf{e}_n | J_k | \mathbf{e}_r \rangle g_{mr} . \quad (\text{D10})$$

In analogy to Eq. (D3) we define the operator

$$\tilde{g}(\theta, \phi) = \exp\{-i\phi\tilde{J}_z\} \exp\{-i\theta\tilde{J}_y\} . \quad (\text{D11})$$

In the body-fixed system, the matrix elements of \tilde{g} are given by

$$\tilde{g}_{\mu\nu} = \langle \mathbf{e}'_\mu | \tilde{g} | \mathbf{e}'_\nu \rangle . \quad (\text{D12})$$

Eq. (D9) implies that the matrix elements $g_{\mu\nu}$ of g in the space-fixed system and $\tilde{g}_{\mu\nu}$ of \tilde{g} in the body-fixed system are equal,

$$g_{\mu\nu} = \tilde{g}_{\mu\nu} . \quad (\text{D13})$$

The equality of these two matrices implies that we may use either form. If the matrix g operates in the space-fixed system we use the form $g_{\mu\nu}$, if it acts in the body-fixed system, we use the form $\tilde{g}_{\mu\nu}$. If we employ an operator representation we proceed likewise and use g as defined in Eq. (D4) in the space-fixed system and \tilde{g} as defined in Eq. (D11) in the body-fixed system.

Let the angles θ, ϕ and, with these, the transformation g be dependent upon time. Let $\mathbf{A} = A_x|\mathbf{e}'_x\rangle + A_y|\mathbf{e}'_y\rangle$ be a vector in the tangential plane (i.e., perpendicular to $|\mathbf{e}'_z\rangle$) with time-dependent components $A_x(t), A_y(t)$. The time derivative of \mathbf{A} , indicated by a dot, is

$$\dot{\mathbf{A}} = \dot{A}_x|\mathbf{e}'_x\rangle + \dot{A}_y|\mathbf{e}'_y\rangle + A_x|\dot{\mathbf{e}}'_x\rangle + A_y|\dot{\mathbf{e}}'_y\rangle . \quad (\text{D14})$$

We use $|\dot{\mathbf{e}}'_k\rangle = \sum_j |\mathbf{e}_j\rangle \dot{g}_{jk} = \sum_{jl} g_{jl} \dot{g}_{jk} |\mathbf{e}'_l\rangle$ and $g_{jl} = g_{lj}^{-1}$. Moreover, from $(d/dt)(g^{-1}g) = 0$ it follows that the matrix $(g^{-1}\dot{g})_{kl}$ is antisymmetric. Thus,

$$|\dot{\mathbf{e}}'_k\rangle = \sum_l (g^{-1}\dot{g})_{lk} |\mathbf{e}'_l\rangle = - \sum_l (g^{-1}\dot{g})_{kl} |\mathbf{e}'_l\rangle . \quad (\text{D15})$$

Explicit calculation shows that

$$g^{-1}\dot{g} \rightarrow \begin{pmatrix} 0 & -\dot{\phi}\cos\theta & \dot{\theta} \\ \dot{\phi}\cos\theta & 0 & \dot{\phi}\sin\theta \\ -\dot{\theta} & -\dot{\phi}\sin\theta & 0 \end{pmatrix} . \quad (\text{D16})$$

Combining Eqs. (D9) to (D11) we obtain

$$\begin{aligned} \dot{\mathbf{A}} &= \dot{A}_x|\mathbf{e}'_x\rangle + \dot{A}_y|\mathbf{e}'_y\rangle + A_x\dot{\phi}\cos\theta|\mathbf{e}'_x\rangle - A_x\dot{\theta}|\mathbf{e}'_z\rangle \\ &\quad - A_y\dot{\phi}\cos\theta|\mathbf{e}'_x\rangle - A_y\dot{\phi}\sin\theta|\mathbf{e}'_z\rangle . \end{aligned} \quad (\text{D17})$$

This is Eq. (C2). The covariant derivative of \mathbf{A} is defined as the projection of $\dot{\mathbf{A}}$ onto the tangential plane,

$$D_t\mathbf{A} = (\dot{A}_x - A_y\dot{\phi}\cos\theta)|\mathbf{e}'_x\rangle + (\dot{A}_y + A_x\dot{\phi}\cos\theta)|\mathbf{e}'_y\rangle . \quad (\text{D18})$$

Using the fact that in the basis $|\mathbf{e}'_k\rangle$ the operators \tilde{J}_k have the matrix representation (D5), we write Eq. (D18) in the form

$$iD_t\mathbf{A} = (i\partial_t + \dot{\phi}\cos\theta\tilde{J}_z)\mathbf{A} . \quad (\text{D19})$$

That agrees with Eq. (38). The partial derivative acts only on the components (A_x, A_y) of \mathbf{A} . The additional term accounts for a rotation around the z' -axis by the angle $\dot{\phi}\cos\theta$. That is the hallmark of a covariant derivative.

Given two vectors $\mathbf{a} = \sum_j a_j(t) |\mathbf{e}_j\rangle$ and $\mathbf{b} = \sum_j b_j(t) |\mathbf{e}_j\rangle$ in the space-fixed system with time-dependent coefficients $a_j(t), b_j(t)$, we transcribe the inner product of \mathbf{b} and of the time derivative $\dot{\mathbf{a}}$ of \mathbf{a} , i.e., the expression $\sum_j b_j \dot{a}_j$, into the body-fixed system. As mentioned earlier we distinguish the system-dependent representations of the two vectors by writing $\mathbf{a} \rightarrow \mathbf{A} = \sum_j A_j |\mathbf{e}'_j\rangle$ and $\mathbf{b} \rightarrow \mathbf{B} = \sum_j B_j |\mathbf{e}'_j\rangle$. To focus attention on the covariant derivative we put $A_z = 0 = B_z$. Then both $\mathbf{A} = A_x|\mathbf{e}'_x\rangle + A_y|\mathbf{e}'_y\rangle$ and $\mathbf{B} = B_x|\mathbf{e}'_x\rangle + B_y|\mathbf{e}'_y\rangle$ are tangential vectors in the body-fixed system. From Eq. (D2) we have $a_j = \sum_k g_{jk} A_k$, $b_j = \sum_k g_{jk} B_k$ and, thus,

$$\begin{aligned} \mathbf{b}\dot{\mathbf{a}} &= \sum_j b_j \dot{a}_j \\ &= \sum_{jkl} B_k g_{jk} \frac{d}{dt} (g_{jl} A_l) \\ &= \sum_k B_k \dot{A}_k + \sum_{kl} B_k A_l (g^{-1}\dot{g})_{kl} \\ &= B_x(\dot{A}_x - \dot{\phi}\cos\theta A_y) + B_y(\dot{A}_y + \dot{\phi}\cos\theta A_x) , \end{aligned} \quad (\text{D20})$$

or, using the definition (D19),

$$\mathbf{b}\dot{\mathbf{a}} = \mathbf{B}D_t\mathbf{A} . \quad (\text{D21})$$

Eq. (D21) gives the rule for transcribing time derivatives of vectors into the body-fixed system. It applies provided in the body-fixed system, the vectors are tangential.

We define an infinitesimal transformation r in the space-fixed system and another infinitesimal transformation \tilde{r} in the body-fixed system. Both are defined in terms of the augmented rotation $g(\theta + \delta\theta, \phi + \delta\phi) \exp\{-iJ_z\gamma\}$. Here $\delta\theta, \delta\phi, \gamma$ are infinitesimal. That changes $g \rightarrow g + \delta g$. In the space-fixed system we consider the infinitesimal transformation δg acting on the vectors $|\mathbf{e}_j\rangle$, keeping the

vectors $|\mathbf{e}'_k\rangle$ fixed. Eqs. (D1) give

$$\begin{aligned} |\delta\mathbf{e}_j\rangle &= \sum_k (\delta g)_{jk} |\mathbf{e}'_k\rangle \\ &= \sum_{kl} (\delta g)_{jk} g_{lk} |\mathbf{e}_l\rangle \\ &= \sum_l (\delta g g^{-1})_{jl} |\mathbf{e}_l\rangle \\ &= \sum_l r_{jl} |\mathbf{e}_l\rangle. \end{aligned} \quad (\text{D22})$$

The last relation defines r . Explicit calculation shows that

$$\begin{aligned} r &= \delta g g^{-1} \\ &= \delta\phi(-iJ_z) + \delta\theta \cos\phi(-iJ_y) \\ &\quad - \delta\theta \sin\phi(-iJ_x) + \gamma \cos\theta(-iJ_z) \\ &\quad + \gamma \sin\theta \cos\phi(-iJ_x) + \gamma \sin\theta \sin\phi(-iJ_y) \end{aligned} \quad (\text{D23})$$

A general infinitesimal transformation in the space-fixed system can be written in terms of infinitesimal angles $\delta\alpha_k$ as

$$r = \sum_k \delta\alpha_k (-iJ_k). \quad (\text{D24})$$

Equating that with r as given in Eq. (D23) we obtain a linear relation between the infinitesimal angles $\delta\theta$, $\delta\phi$, γ and the angles $\delta\alpha_k$. It reads

$$\begin{pmatrix} \delta\alpha_x \\ \delta\alpha_y \\ \delta\alpha_z \end{pmatrix} = \begin{pmatrix} -\sin\phi & 0 & \sin\theta \cos\phi \\ \cos\phi & 0 & \sin\theta \sin\phi \\ 0 & 1 & \cos\theta \end{pmatrix} \begin{pmatrix} \delta\theta \\ \delta\phi \\ \gamma \end{pmatrix}. \quad (\text{D25})$$

The inverse relation is

$$\begin{pmatrix} \delta\theta \\ \delta\phi \\ \gamma \end{pmatrix} = \begin{pmatrix} -\sin\phi & \cos\phi & 0 \\ -\cos\phi \cot\theta & -\sin\phi \cot\theta & 1 \\ \frac{\cos\phi}{\sin\theta} & \frac{\sin\phi}{\sin\theta} & 0 \end{pmatrix} \begin{pmatrix} \delta\alpha_x \\ \delta\alpha_y \\ \delta\alpha_z \end{pmatrix}. \quad (\text{D26})$$

Identifying γ with $\delta\omega$, we see that this agrees with Eqs. (B3) and (B4). In the body-fixed system we consider the infinitesimal transformation $(\delta g)^{-1}$ acting on the vectors $|\mathbf{e}'_k\rangle$, keeping the vectors $|\mathbf{e}_j\rangle$ fixed. Equations (D1) give

$$\begin{aligned} |\delta\mathbf{e}'_k\rangle &= \sum_j (\delta g^{-1})_{kj} |\mathbf{e}_j\rangle \\ &= \sum_{jl} (\delta g^{-1})_{kj} g_{jl} |\mathbf{e}'_l\rangle \\ &= \sum_l [(\delta g)^{-1}g]_{kl} |\mathbf{e}'_l\rangle \\ &= \sum_l \tilde{r}_{kl} |\mathbf{e}'_l\rangle. \end{aligned} \quad (\text{D27})$$

The last relation defines \tilde{r} . Eqs. (D27) show that \tilde{r} acts in the body-fixed system. We use the arguments below

Eq. (D13) to express \tilde{r} in terms of the operator \tilde{g} defined in Eq. (D11). Explicit calculation shows that

$$\begin{aligned} \tilde{r} &= (\delta\tilde{g})^{-1}\tilde{g} \\ &= -\delta\phi \cos\theta(-i\tilde{J}_z) - \delta\theta(-i\tilde{J}_y) \\ &\quad + \delta\phi \sin\theta(-i\tilde{J}_x) - \gamma(-i\tilde{J}_z). \end{aligned} \quad (\text{D28})$$

Since $\delta(\tilde{g}^{-1}\tilde{g}) = 0$ we have $(\delta\tilde{g}^{-1})\tilde{g} = -\tilde{g}^{-1}\delta\tilde{g}$. The last relation shows that the three infinitesimal angles $\delta\theta$, $\delta\phi$, γ all carry negative signs. That is because the infinitesimal transformation $\delta\tilde{g}^{-1}$ acts conversely to the infinitesimal transformation $\delta\tilde{g}$. A general infinitesimal transformation in the body-fixed system can be written in terms of infinitesimal angles $\delta\tilde{\alpha}_k$ as

$$\tilde{r} = \sum_k \delta\tilde{\alpha}_k (-i\tilde{J}_k). \quad (\text{D29})$$

Since in Eq. (D28) \tilde{r} acts conversely to r we equate expression (D28) not with expression (D29) but with the converse of expression (D29), obtained by the replacements $\delta\tilde{\alpha}_k \rightarrow -\delta\tilde{\alpha}_k$ for all k . That gives

$$\begin{pmatrix} \delta\tilde{\alpha}_x \\ \delta\tilde{\alpha}_y \\ \delta\tilde{\alpha}_z \end{pmatrix} = \begin{pmatrix} 0 & -\sin\theta & 0 \\ 1 & 0 & 0 \\ 0 & \cos\theta & 1 \end{pmatrix} \begin{pmatrix} \delta\theta \\ \delta\phi \\ \gamma \end{pmatrix}. \quad (\text{D30})$$

The inverse relation is

$$\begin{pmatrix} \delta\theta \\ \delta\phi \\ \gamma \end{pmatrix} = \begin{pmatrix} 0 & 1 & 0 \\ -\frac{1}{\sin\theta} & 0 & 0 \\ \cot\theta & 0 & 1 \end{pmatrix} \begin{pmatrix} \delta\tilde{\alpha}_x \\ \delta\tilde{\alpha}_y \\ \delta\tilde{\alpha}_z \end{pmatrix}. \quad (\text{D31})$$

Identifying γ with $\delta\omega$, we see that this agrees with Eqs. (B10) and (B11).

The commutation relations (D4) imply that under the infinitesimal rotation $1 + \delta\alpha_z(-iJ_z)$, the operator $(-iJ_x)$ is mapped onto $[1 + \delta\alpha_z(-iJ_z)](-iJ_x)[1 - \delta\alpha_z(-iJ_z)] = (-iJ_x) + \delta\alpha_z(-iJ_y)$, and correspondingly for the other components. That shows that under a rotation, the three operators $(-iJ_x, -iJ_y, -iJ_z)$ transform like the three unit vectors $(\mathbf{e}_x, \mathbf{e}_y, \mathbf{e}_z)$ of a three-dimensional linear space. That suggests that r in Eq. (D24) and \tilde{r} in Eq. (D29) represent the same vector written, respectively, in the space-fixed and in the body-fixed coordinate system. For that to be true the three infinitesimal angles $(\delta\alpha_x, \delta\alpha_y, \delta\alpha_z)$ of r and $(\delta\tilde{\alpha}_x, \delta\tilde{\alpha}_y, \delta\tilde{\alpha}_z)$ of \tilde{r} must be connected as in Eq. (D2),

$$\delta\alpha_k = \sum_l g_{kl} \delta\tilde{\alpha}_l. \quad (\text{D32})$$

Combining Eqs. (D25) and (D31) yields

$$\begin{aligned} &\begin{pmatrix} \delta\alpha_x \\ \delta\alpha_y \\ \delta\alpha_z \end{pmatrix} \\ &= \begin{pmatrix} \cos\theta \cos\phi & -\sin\phi & \sin\theta \cos\phi \\ \cos\theta \sin\phi & \cos\phi & \sin\theta \sin\phi \\ -\sin\theta & 0 & \cos\theta \end{pmatrix} \begin{pmatrix} \delta\tilde{\alpha}_x \\ \delta\tilde{\alpha}_y \\ \delta\tilde{\alpha}_z \end{pmatrix}. \end{aligned} \quad (\text{D33})$$

Equation (D7) shows that Eq. (D33) indeed equals Eq. (D32), confirming the vector character of r . Applying that to Noether's theorem in App. B 3 we see that I_k and $I_{k'}$ are indeed the components of the same vector written respectively, in the space-fixed and in the body-fixed coordinate system.

It is straightforward to extend these arguments from vectors, i.e. spherical tensors of rank three, to spherical tensors of arbitrary rank. Then, the concrete representations of the rotation matrices g and \tilde{g} are given by Wigner D matrices, while all algebraic relationships derived above remain unchanged.

Appendix E: Gauge potentials

We demonstrate how gauge potentials arise in an adiabatic approach and we discuss gauge transformations and their relation to rotations.

1. Gauge potentials from an adiabatic approach

The appearance of the non-Abelian gauge potential (40) can be understood also in an adiabatic approach [65, 79]. If the nucleon's degrees of freedom are much faster than those of the rotor, the eigenstates of the fermion Hamiltonian H_Ψ follow the rotor's axial symmetry instantaneously, independently of any details of the fermion-rotor interaction. For simplicity we consider only the fermion spin function $\chi_{S m}$ with half-integer spin S and projection m onto the space-fixed z axis. As the fermion is fast, it's spin is in an eigenstate with respect to projection onto the rotor's symmetry axis, i.e. the helicity spin states $\chi_{S\lambda}(\theta, \phi)$ from Eq. (C4) span, for fixed projection λ , a basis of the instantaneous fermion eigenstates. They fulfill

$$(\mathbf{e}_r \cdot \mathbf{S}) \chi_{S\lambda}(\theta, \phi) = \lambda \chi_{S\lambda}(\theta, \phi). \quad (\text{E1})$$

Due to Kramers' degeneracy, the spin states $\chi_{S\pm\lambda}(\theta, \phi)$ are degenerate. In the adiabatic approximation, one evaluates the Hamiltonian of the fermion-plus-rotor system

$$H = H_\Psi - \frac{1}{2C_0} \nabla_\Omega^2, \quad (\text{E2})$$

in these eigenstates to get the effective Hamiltonian matrix (see, e.g., Berry's overview in Ref. [79])

$$\begin{aligned} H_{S'S} &\equiv \chi_{S'\lambda}^\dagger(\theta, \phi) H \chi_{S\lambda}(\theta, \phi) \\ &= \frac{1}{2C_0} (-i\delta_{S'S'} \nabla_\Omega - \mathbf{A}_{S'S})^2 \\ &\quad + \chi_{S\lambda}^\dagger(\theta, \phi) H_\Psi \chi_{S\lambda}(\theta, \phi). \end{aligned} \quad (\text{E3})$$

Here the vector gauge potential is the matrix

$$\mathbf{A}_{S'S} \equiv i\chi_{S'\lambda}^\dagger(\theta, \phi) \nabla_\Omega \chi_{S\lambda}(\theta, \phi). \quad (\text{E4})$$

Using properties of Wigner D functions [52] and a summation formula from Ref. [80], one finds

$$\mathbf{A}_{S'S} = \delta_{S'S} \lambda \cot \theta \mathbf{e}_\phi. \quad (\text{E5})$$

In our case, the projection λ is obtained by application of the operator $\hat{K}_{z'}$, and we thus find that the gauge potential $\mathbf{A} = \mathbf{e}_\phi \cot \theta \hat{K}_{z'}$ enters. This is Eq. (40).

2. Gauge transformations

Let us also explore gauge transformations. Our definition of the body-fixed coordinate system (7) is convenient [because the basis vectors \mathbf{e}_θ and \mathbf{e}_ϕ are tangent vectors of the lines parameterized by the spherical coordinates (θ, ϕ)] but otherwise arbitrary. Any rotation of these basis vectors around the \mathbf{e}_r axis would have been equally valid, i.e. the vectors

$$\begin{aligned} \mathbf{e}'_1 &\equiv \cos \gamma(\theta, \phi) \mathbf{e}_\theta + \sin \gamma(\theta, \phi) \mathbf{e}_\phi, \\ \mathbf{e}'_2 &\equiv -\sin \gamma(\theta, \phi) \mathbf{e}_\theta + \cos \gamma(\theta, \phi) \mathbf{e}_\phi, \end{aligned} \quad (\text{E6})$$

and \mathbf{e}_r span a right-handed body-fixed coordinate system. Here, $\gamma(\theta, \phi)$ is a smooth function over the sphere. Let us repeat the computations made in the previous Subsection for this body-fixed system. The helicity basis functions for the fermion become

$$\tilde{\chi}_{S\lambda}(\theta, \phi) = \sum_m D_{m\lambda}^S(\phi, \theta, \gamma) \chi_{S m}. \quad (\text{E7})$$

Here, and in what follows we suppress the dependence of γ on the angles (θ, ϕ) . The gauge potential is

$$\begin{aligned} \tilde{\mathbf{A}}_{S'S} &\equiv i\tilde{\chi}_{S'\lambda}^\dagger(\theta, \phi) \nabla_\Omega \tilde{\chi}_{S\lambda}(\theta, \phi) \\ &= i\delta_{S'S'} \sum_m [D_{m\lambda}^S(\phi, \theta, \gamma)]^* \nabla_\Omega D_{m\lambda}^S(\phi, \theta, \gamma) \\ &= i\delta_{S'S'} \sum_m d_{m\lambda}^S(\theta) \left[\left(\frac{-im}{\sin \theta} \mathbf{e}_\phi - i\lambda \nabla_\Omega \gamma \right) d_{m\lambda}^S(\theta) \right. \\ &\quad \left. - \frac{1}{2} \sqrt{S(S+1) - m(m-1)} d_{m-1\lambda}^S(\theta) \mathbf{e}_\theta \right. \\ &\quad \left. + \frac{1}{2} \sqrt{S(S+1) - m(m+1)} d_{m+1\lambda}^S(\theta) \mathbf{e}_\theta \right] \\ &= \delta_{S'S} \lambda [\cot \theta \mathbf{e}_\phi + \nabla_\Omega \gamma(\theta, \phi)]. \end{aligned} \quad (\text{E8})$$

We have used results from chapter 4.9 of Ref. [52]. The sums over the last two terms cancel each other, and we used $\sum_m m [d_{m\lambda}^S(\theta)]^2 = \lambda \cos \theta$ and $\sum_m [d_{m\lambda}^S(\theta)]^2 = 1$ from Ref. [80].

The vector potentials $\tilde{\mathbf{A}}_{S'S}$ and $\mathbf{A}_{S'S}$ differ by a gauge transformation, which is generated by the arbitrary angle $\gamma(\theta, \phi)$. For $\gamma(\theta, \phi) = \pm\phi$, for instance, one obtains the gauge potentials $\tilde{\mathbf{A}} = \lambda \frac{\cos \theta \pm 1}{\sin \theta} \mathbf{e}_\phi$ by Wu and Yang [69]. Another interesting choice is $\gamma(\theta, \phi) = -\phi \cos \theta$, because it generates the non-singular gauge potential $\tilde{\mathbf{A}} = \lambda \phi \sin \theta \mathbf{e}_\theta$. Our gauge potential (40) is singular at both poles, and the rotor eigenfunctions are Wigner D

functions. As pointed out in Ref. [81], the different gauge potentials correspond to different conventions regarding the third argument of the Wigner D function, i.e. to different conventions regarding rotations of the body-fixed coordinate system around its z' axis. In other words, the wave function $D_{MK}^I(\phi, \theta, 0)$ we used in the main text is replaced by $D_{MK}^I[\phi, \theta, \gamma(\theta, \phi)]$ when a gauge transformation is made.

The arguments of this Subsection show that the freedom of choice of the intrinsic coordinate system introduces a gauge freedom in the dynamics of the collective rotational degrees of freedom [53]. The general Abelian gauge potential is

$$\tilde{\mathbf{A}}_a(\theta, \phi) = \hat{K}_{z'} [\mathbf{e}_\phi \cot \theta + \nabla_\Omega \gamma(\theta, \phi)] . \quad (\text{E9})$$

We extend the discussion to the non-Abelian gauge field. In its manifestly gauge-invariant form it reads

$$\begin{aligned} \tilde{\mathbf{A}}_n(\theta, \phi) &= g \mathbf{e}_r \times \hat{\mathbf{K}} \\ &= g \left(\hat{K}_1 \mathbf{e}'_2 - \hat{K}_2 \mathbf{e}'_1 \right) \\ &= g \left[\left(\hat{K}_1 \cos \gamma(\theta, \phi) - \hat{K}_2 \sin \gamma(\theta, \phi) \right) \mathbf{e}_\phi \right. \\ &\quad \left. - \left(\hat{K}_1 \sin \gamma(\theta, \phi) + \hat{K}_2 \cos \gamma(\theta, \phi) \right) \mathbf{e}_\theta \right] . \end{aligned} \quad (\text{E10})$$

We have employed the operators $\hat{K}_i \equiv \mathbf{e}'_i \cdot \hat{\mathbf{K}}$ for $i = 1, 2$ in the body-fixed frame. In the last line we have expressed the result in the coordinate system of the rotor's angular velocity. We have used that the spin operators \hat{K}_1 , \hat{K}_2 , and $\hat{K}_{z'}$ fulfill the canonical commutation relations. Comparison with Eq. (43) meets our expectations, because the spin operators are simply rotated by γ around the body-fixed z' axis.

The magnetic field of the total gauge potential $\tilde{\mathbf{A}}_{\text{tot}} = \tilde{\mathbf{A}}_a + \tilde{\mathbf{A}}_n$ is

$$\begin{aligned} \tilde{\mathbf{B}}_{\text{tot}} &= \nabla_\Omega \times \tilde{\mathbf{A}}_{\text{tot}} - i \tilde{\mathbf{A}}_{\text{tot}} \times \tilde{\mathbf{A}}_{\text{tot}} \\ &= (g^2 - 1) \hat{K}_{z'} \mathbf{e}_r , \end{aligned} \quad (\text{E11})$$

in agreement with Eq. (46). It does not depend on $\gamma(\theta, \phi)$ and is, thus, gauge invariant.

We turn this argument around and study the effect of rotations on the gauge potential. While the non-Abelian part (E10) of the gauge potential is manifestly invariant under rotations, this is not so for the Abelian part (40). Under a rotation we have

$$\begin{aligned} \mathcal{R} \mathbf{A}_a(\theta, \phi) &= \\ \hat{K}_{z'} \cot \theta [\mathbf{e}_\phi(\phi + \delta\phi, \theta + \delta\theta) - \delta\omega \mathbf{e}_\theta(\phi + \delta\phi, \theta + \delta\theta)] . \end{aligned} \quad (\text{E12})$$

Here, the differential $\delta\omega$ is given in Eq. (B4) for rotations around the space-fixed axes. This rotated gauge potential has to be compared with the gauge potential

$$\begin{aligned} \mathbf{A}_a(\theta + \delta\theta, \phi + \delta\phi) &= \\ \hat{K}_{z'} \cot(\theta + \delta\theta) \mathbf{e}_\phi(\phi + \delta\phi, \theta + \delta\theta) \end{aligned} \quad (\text{E13})$$

at the point $(\phi + \delta\phi, \theta + \delta\theta)$. Here, the differential $\delta\theta$ is taken from Eq. (B3). The difference

$$\begin{aligned} \delta \mathbf{A} &= \mathcal{R} \mathbf{A}_a(\theta) - \mathbf{A}_a(\theta + \delta\theta) \\ &= -\delta\omega \cot \theta \hat{K}_{z'} \mathbf{e}_\theta(\phi + \delta\phi, \theta + \delta\theta) \\ &\quad + \delta\theta \frac{\hat{K}_{z'}}{\sin^2 \theta} \mathbf{e}_\phi(\phi + \delta\phi, \theta + \delta\theta) \end{aligned} \quad (\text{E14})$$

can be written as $\delta \mathbf{A} = \nabla_\Omega \hat{K}_{z'} \delta\omega$ when employing the expressions (B3) and (B4). Thus, after a rotation the gauge potential can be brought back into its original form (45) by performing a gauge transformation [68].

Appendix F: Supplements to Section (IV)

To compute the contribution of the term linear in g of the Hamiltonian (60) for $K = 1/2$ states we introduce spherical components

$$\begin{aligned} I_{\pm 1} &\equiv \mp \frac{1}{\sqrt{2}} (I_{x'} \pm i I_{y'}) \\ &= \frac{i}{\sqrt{2}} \left(i \partial_\theta \mp \frac{1}{\sin \theta} \partial_\phi \pm i \hat{K}_{z'} \cot \theta \right) \end{aligned} \quad (\text{F1})$$

and

$$\hat{K}_{\pm 1} \equiv \mp \frac{1}{\sqrt{2}} \left(\hat{K}_{x'} \pm i \hat{K}_{y'} \right) . \quad (\text{F2})$$

We write the term as

$$\frac{g}{C_0} \left(I_{x'} \hat{K}_{x'} + I_{y'} \hat{K}_{y'} \right) = -\frac{g}{C_0} \left(I_{-1} \hat{K}_{+1} + I_{+1} \hat{K}_{-1} \right) . \quad (\text{F3})$$

Using the properties of the raising and lowering operators (see chapters 3.1 and 4.2 in Ref. [52]) we find

$$\hat{K}_{\pm 1} \left| \mp \frac{1}{2} \right\rangle = \mp \frac{1}{\sqrt{2}} \left| \pm \frac{1}{2} \right\rangle , \quad (\text{F4})$$

and

$$\begin{aligned} I_{\pm 1} D_{M, M'}^I(\phi, \theta, 0) &= \\ \pm \sqrt{\frac{I(I+1) - M'(M' \pm 1)}{2}} D_{M, M' \pm 1}^I(\phi, \theta, 0) . \end{aligned} \quad (\text{F5})$$

Thus,

$$\begin{aligned} \left(I_{-1} \hat{K}_{+1} + I_{+1} \hat{K}_{-1} \right) D_{M, \pm \frac{1}{2}}^I(\phi, \theta, 0) \left| \mp \frac{1}{2} \right\rangle &= \\ \left(I + \frac{1}{2} \right) D_{M, \mp \frac{1}{2}}^I(\phi, \theta, 0) \left| \pm \frac{1}{2} \right\rangle . \end{aligned} \quad (\text{F6})$$

Inspection shows that that the linear combinations

$$D_{M, -\frac{1}{2}}^I(\phi, \theta, 0) \left| \frac{1}{2} \right\rangle + (-1)^{I+\frac{1}{2}} D_{M, \frac{1}{2}}^I(\phi, \theta, 0) \left| -\frac{1}{2} \right\rangle \quad (\text{F7})$$

are solutions of the Hamiltonian (60) for $K = 1/2$. The phase $(-1)^{I+\frac{1}{2}}$ results from the requirement that the odd-mass nucleus is invariant under rotations by π around any axis perpendicular to the symmetry axis. Hence, the contribution from the term proportional to g in the Hamiltonian (60) becomes

$$\Delta E(g) = -\frac{g}{C_0} \delta_{|K|}^{\frac{1}{2}} (-1)^{I+\frac{1}{2}} \left(I + \frac{1}{2} \right). \quad (\text{F8})$$

That yields Eq. (69).

We next compute the matrix elements of the g -dependent terms of the Hamiltonian (60) for two close-lying band heads. Using the normalization to $4\pi/(2I+1)$ of the squared Wigner function, see Chapter 4.11 of Ref. [52], we find

$$\begin{aligned} & \int_0^{2\pi} d\phi \int_{-1}^1 d \cos \theta \langle K | [D_{M,-K}^I(\phi, \theta, 0)]^* I_{+1} \hat{K}_{-1} \\ & D_{M,-K-1}^I(\phi, \theta, 0) | K+1 \rangle \\ & = \langle K | \hat{K}_{-1} | K+1 \rangle \\ & \times \int_0^{2\pi} d\phi \int_{-1}^1 d \cos \theta D_{M,-K}^{I*}(\phi, \theta, 0) I_{+1} D_{M,-K-1}^I(\phi, \theta, 0) \\ & = \frac{4\pi}{2I+1} \sqrt{\frac{I(I+1) - K(K+1)}{2}} \langle K | \hat{K}_{-1} | K+1 \rangle. \end{aligned} \quad (\text{F9})$$

We have used Eq. (F5). The other relevant matrix element is

$$\begin{aligned} & \int_0^{2\pi} d\phi \int_{-1}^1 d \cos \theta \langle -K | [D_{M,K}^I(\phi, \theta, 0)]^* I_{-1} \hat{K}_{+1} \\ & D_{M,K+1}^I(\phi, \theta, 0) | -K-1 \rangle \\ & = \langle -K | \hat{K}_{+1} | -K-1 \rangle \\ & \times \int_0^{2\pi} d\phi \int_{-1}^1 d \cos \theta D_{M,K}^{I*}(\phi, \theta, 0) I_{-1} D_{M,K+1}^I(\phi, \theta, 0) \\ & = \frac{-4\pi}{2I+1} \sqrt{\frac{I(I+1) - K(K+1)}{2}} \langle -K | \hat{K}_{+1} | -K-1 \rangle. \end{aligned} \quad (\text{F10})$$

Time-reversal invariance relates both matrix elements. Denoting the time-reversal operator by \mathcal{T} we have

$$\begin{aligned} \langle -K | \hat{K}_{+1} | -K-1 \rangle & = \langle K | \mathcal{T}^\dagger \hat{K}_{+1} \mathcal{T} | K+1 \rangle \\ & = -\langle K | \hat{K}_{-1} | K+1 \rangle. \end{aligned} \quad (\text{F11})$$

The interaction is characterized by a single parameter. For a given potential V , the relevant matrix element can be calculated by expanding the axially symmetric eigenstates in terms of spherical basis functions. In our approach, $\langle K | \hat{K}_{-1} | K+1 \rangle$ is a low-energy constant and needs to be adjusted to data.

The next-to-leading-order correction of the Hamiltonian is

$$\begin{aligned} H_{\text{NLO}} & = -\frac{1}{2} \left(p_\theta + g \hat{K}_{y'}, p_\phi - \cos \theta \hat{K}_{z'} - g \sin \theta \hat{K}_{x'} \right) \\ & \times \hat{M}_{\text{LO}}^{-1} \hat{M}_{\text{NLO}} \hat{M}_{\text{LO}}^{-1} \begin{pmatrix} p_\theta + g \hat{K}_{y'} \\ p_\phi - \cos \theta \hat{K}_{z'} - g \sin \theta \hat{K}_{x'} \end{pmatrix}. \end{aligned} \quad (\text{F12})$$

Here, the ‘‘mass’’ matrices

$$\hat{M}_{\text{LO}} = \frac{1}{C_0} \begin{bmatrix} 1 & 0 \\ 0 & \sin^2 \theta \end{bmatrix} \quad (\text{F13})$$

and

$$\begin{aligned} \hat{M}_{\text{NLO}} & = \left(g_a \left(\hat{K}_{x'}^2 + \hat{K}_{y'}^2 \right) + g_b \hat{K}_{z'}^2 \right) \begin{bmatrix} 1 & 0 \\ 0 & \sin^2 \theta \end{bmatrix} \\ & + g_c \begin{bmatrix} \hat{K}_{x'}^2 & \hat{K}_{x'} \hat{K}_{y'} \sin \theta \\ \hat{K}_{y'} \hat{K}_{x'} \sin \theta & \hat{K}_{y'}^2 \sin^2 \theta \end{bmatrix} \end{aligned} \quad (\text{F14})$$

enter the perturbative inversion of the mass matrix

$$\hat{M} = \hat{M}_{\text{LO}} + \hat{M}_{\text{NLO}} \quad (\text{F15})$$

via

$$\hat{M}^{-1} \approx \hat{M}_{\text{LO}}^{-1} - \hat{M}_{\text{LO}}^{-1} \hat{M}_{\text{NLO}} \hat{M}_{\text{LO}}^{-1}. \quad (\text{F16})$$

The resulting Hamiltonian is written as in Eq. (73). Using Eq. (57) we replace the canonical momenta by angular momentum components,

$$\begin{aligned} p_\theta & = I_{y'} , \\ \frac{p_\phi}{\sin \theta} & = \hat{K}_{z'} \cot \theta - I_{x'} , \end{aligned} \quad (\text{F17})$$

and find

$$\begin{aligned} \hat{C} & \equiv -\frac{\left(g_a + \frac{g_c}{2} \right) \left(\hat{K}_{x'}^2 + \hat{K}_{y'}^2 \right) + g_b \hat{K}_{z'}^2}{C_0} \begin{bmatrix} 1 & 0 \\ 0 & 1 \end{bmatrix}, \\ \hat{G} & \equiv -\frac{g_c}{C_0} \begin{bmatrix} \frac{1}{2} \left(\hat{K}_{x'}^2 - \hat{K}_{y'}^2 \right) & \hat{K}_{x'} \hat{K}_{y'} \\ \hat{K}_{y'} \hat{K}_{x'} & \frac{1}{2} \left(\hat{K}_{y'}^2 - \hat{K}_{x'}^2 \right) \end{bmatrix}, \end{aligned} \quad (\text{F18})$$

and

$$\mathbf{N} \equiv \begin{pmatrix} I_{y'} \\ I_{x'} \end{pmatrix} + g \begin{pmatrix} \hat{K}_{y'} \\ \hat{K}_{x'} \end{pmatrix}. \quad (\text{F19})$$

With a view on Eq. (73) we note that

$$\begin{aligned} \mathbf{N}^T \mathbf{N} & = \left(I_{x'} + g \hat{K}_{x'} \right)^2 + \left(I_{y'} + g \hat{K}_{y'} \right)^2 \\ & = \mathbf{I}^2 - \hat{K}_{z'}^2 + g^2 \left(\hat{K}_{x'}^2 + \hat{K}_{y'}^2 \right) \\ & + 2g \left(I_{x'} \hat{K}_{x'} + I_{y'} \hat{K}_{y'} \right), \end{aligned} \quad (\text{F20})$$

and this expression is familiar to us from the leading-order Hamiltonian (60). This makes it straight forward to evaluate the next-to-leading-order corrections.

-
- [1] P. F. Bedaque and U. van Kolck, “Effective field theory for few-nucleon systems,” *Annual Review of Nuclear and Particle Science* **52**, 339–396 (2002), nucl-th/0203055.
- [2] S. K. Bogner, T. T. S. Kuo, and A. Schwenk, “Model-independent low momentum nucleon interaction from phase shift equivalence,” *Physics Reports* **386**, 1 – 27 (2003).
- [3] E. Epelbaum, H.-W. Hammer, and Ulf-G. Meißner, “Modern theory of nuclear forces,” *Rev. Mod. Phys.* **81**, 1773–1825 (2009).
- [4] S.K. Bogner, R.J. Furnstahl, and A. Schwenk, “From low-momentum interactions to nuclear structure,” *Prog. Part. Nucl. Phys.* **65**, 94 – 147 (2010).
- [5] H. W. Griebhammer, J. A. McGovern, D. R. Phillips, and G. Feldman, “Using effective field theory to analyse low-energy Compton scattering data from protons and light nuclei,” *Prog. Part. Nucl. Phys.* **67**, 841 – 897 (2012).
- [6] H.-W. Hammer, C. Ji, and D. R. Phillips, “Effective field theory description of halo nuclei,” *Journal of Physics G: Nuclear and Particle Physics* **44**, 103002 (2017).
- [7] P. F. Bedaque, H.-W. Hammer, and U. van Kolck, “Renormalization of the three-body system with short-range interactions,” *Phys. Rev. Lett.* **82**, 463–467 (1999).
- [8] R. J. Furnstahl and H.-W. Hammer, “Are occupation numbers observable?” *Physics Letters B* **531**, 203 – 208 (2002).
- [9] E. R. Anderson, S. K. Bogner, R. J. Furnstahl, and R. J. Perry, “Operator evolution via the similarity renormalization group: The deuteron,” *Phys. Rev. C* **82**, 054001 (2010).
- [10] M. R. Schindler and D. R. Phillips, “Bayesian methods for parameter estimation in effective field theories,” *Ann. Phys.* **324**, 682 – 708 (2009).
- [11] R. J. Furnstahl, D. R. Phillips, and S. Wesolowski, “A recipe for eft uncertainty quantification in nuclear physics,” *Journal of Physics G: Nuclear and Particle Physics* **42**, 034028 (2015).
- [12] T. Papenbrock, “Effective theory for deformed nuclei,” *Nucl. Phys. A* **852**, 36 – 60 (2011).
- [13] T. Papenbrock and H. A. Weidenmüller, “Effective field theory for finite systems with spontaneously broken symmetry,” *Phys. Rev. C* **89**, 014334 (2014).
- [14] T Papenbrock and H A Weidenmüller, “Effective field theory of emergent symmetry breaking in deformed atomic nuclei,” *Journal of Physics G: Nuclear and Particle Physics* **42**, 105103 (2015).
- [15] T. Papenbrock and H. A. Weidenmüller, “Effective field theory for deformed atomic nuclei,” *Physica Scripta* **91**, 053004 (2016).
- [16] Q. B. Chen, N. Kaiser, Ulf-G. Meißner, and J. Meng, “Effective field theory for triaxially deformed nuclei,” *The European Physical Journal A* **53**, 204 (2017).
- [17] Q. B. Chen, N. Kaiser, Ulf-G. Meißner, and J. Meng, “Effective field theory for collective rotations and vibrations of triaxially deformed nuclei,” *Phys. Rev. C* **97**, 064320 (2018).
- [18] Q. B. Chen, N. Kaiser, Ulf-G. Meißner, and J. Meng, “Effective field theory for triaxially deformed odd-mass nuclei,” arXiv e-prints, arXiv:2003.04065 (2020), 2003.04065.
- [19] E. A. Coello Pérez and T. Papenbrock, “Effective field theory for nuclear vibrations with quantified uncertainties,” *Phys. Rev. C* **92**, 064309 (2015).
- [20] E. A. Coello Pérez and T. Papenbrock, “Effective field theory for vibrations in odd-mass nuclei,” *Phys. Rev. C* **94**, 054316 (2016).
- [21] Judah M. Eisenberg and Walter Greiner, *Nuclear Models: Collective and Single-Particle Phenomena* (North-Holland Publishing Company Ltd., London, 1970).
- [22] A. Bohr and B. R. Mottelson, *Nuclear Structure*, Vol. II: Nuclear Deformation (W. A. Benjamin, Reading, Massachusetts, USA, 1975).
- [23] F. Iachello and A. Arima, *The Interacting Boson Model* (Cambridge University Press, Cambridge, UK, 1987).
- [24] G. Herzberg, *Molecular spectra and molecular structure*, Vol. II: Infrared and Raman spectra of polyatomic molecules (Van Nostrand, New York, 1945).
- [25] Aage Bohr, “The coupling of nuclear surface oscillations to the motion of individual nucleons,” *Dan. Mat. Fys. Medd.* **26**, no. 14 (1952).
- [26] Aage Bohr and Ben R. Mottelson, “Collective and individual-particle aspects of nuclear structure,” *Dan. Mat. Fys. Medd.* **27**, no. 16 (1953).
- [27] S. G. Nilsson, “Binding states of individual nucleons in strongly deformed nuclei,” *K. Dan. Vidensk. Selsk. Mat. Fys. Medd.* **29**, no. 16 (1955).
- [28] A. K. Kerman, “Rotational perturbations in nuclei – application to wolfram 183,” *Dan. Mat. Fys. Medd.* **30**, no. 15 (1956).
- [29] David J. Rowe, *Nuclear Collective Motion: Models and Theory*, reprinted ed. (World Scientific, Singapore, 2010).
- [30] P. Ring and P. Schuck, *The Nuclear Many-Body Problem* (Springer, Heidelberg, 1980).
- [31] David J. Rowe and John L. Wood, *Fundamentals of Nuclear Models*, Vol. I: Foundational Models (World Scientific, Singapore, 2010).
- [32] Barry Simon, “Holonomy, the Quantum Adiabatic Theorem, and Berry’s Phase,” *Phys. Rev. Lett.* **51**, 2167–2170 (1983).
- [33] Michael Victor Berry, “Quantal phase factors accompanying adiabatic changes,” *Proceedings of the Royal Society of London. A. Mathematical and Physical Sciences* **392**, 45–57 (1984).
- [34] Frank Wilczek and A. Zee, “Appearance of gauge structure in simple dynamical systems,” *Phys. Rev. Lett.* **52**, 2111–2114 (1984).
- [35] R. Jackiw, “Angular momentum for diatoms described by gauge fields,” *Phys. Rev. Lett.* **56**, 2779–2780 (1986).
- [36] A. Bohm, B. Kendrick, Mark E. Loewe, and L. J. Boya, “The Berry connection and Born-Oppenheimer method,” *Journal of Mathematical Physics* **33**, 977–989 (1992).
- [37] B. Estienne, S. M. Haaker, and K. Schoutens, “Particles in non-Abelian gauge potentials: Landau problem and insertion of non-Abelian flux,” *New Journal of Physics* **13**, 045012 (2011).
- [38] R. S. Nikam and P. Ring, “Manifestation of the Berry phase in diabatic pair transfer in rotating nuclei,” *Phys. Rev. Lett.* **58**, 980–983 (1987).
- [39] Aurel Bulgac, “Time-dependent hartree-fock-bogoliubov approximation and nonintegrable quantum phase,” *Phys. Rev. C* **41**, 2333–2339 (1990).

- [40] Abraham Klein and Niels R. Walet, “Quantum theory of large amplitude collective motion and the born-oppenheimer method,” *Phys. Rev. C* **48**, 178–191 (1993).
- [41] W. Nazarewicz, “Microscopic origin of nuclear deformations,” *Nuclear Physics A* **574**, 27 – 49 (1994).
- [42] Akihisa Hayashi, “Berry phase and decoupling phenomena in $k = 1/2$ nuclear rotational bands,” *Phys. Rev. C* **56**, 2326–2328 (1997).
- [43] S. Chandrasekharan, F.-J. Jiang, M. Pepe, and U.-J. Wiese, “Rotor spectra, berry phases, and monopole fields: From antiferromagnets to qcd,” *Phys. Rev. D* **78**, 077901 (2008).
- [44] E. A. Coello Pérez and T. Papenbrock, “Effective theory for the nonrigid rotor in an electromagnetic field: Toward accurate and precise calculations of $e2$ transitions in deformed nuclei,” *Phys. Rev. C* **92**, 014323 (2015).
- [45] C. Yannouleas and U. Landman, “Symmetry breaking and quantum correlations in finite systems: studies of quantum dots and ultracold bose gases and related nuclear and chemical methods,” *Rep. Prog. Phys.* **70**, 2067 (2007).
- [46] Steven Weinberg, “Nonlinear realizations of chiral symmetry,” *Phys. Rev.* **166**, 1568–1577 (1968).
- [47] S. Coleman, J. Wess, and Bruno Zumino, “Structure of phenomenological lagrangians. i,” *Phys. Rev.* **177**, 2239–2247 (1969).
- [48] Curtis G. Callan, Sidney Coleman, J. Wess, and Bruno Zumino, “Structure of phenomenological lagrangians. ii,” *Phys. Rev.* **177**, 2247–2250 (1969).
- [49] H. Leutwyler, “Nonrelativistic effective lagrangians,” *Phys. Rev. D* **49**, 3033–3043 (1994).
- [50] S. Weinberg, *The Quantum Theory of Fields*, Vol. II (Cambridge University Press, Cambridge, UK, 1996).
- [51] T. Brauner, “Spontaneous symmetry breaking and nambu-goldstone bosons in quantum many-body systems,” *Symmetry* **2**, 609–657 (2010), arXiv:1001.5212.
- [52] D. A. Varshalovich, A. N. Moskalev, and V. K. Kher-sonskii, *Quantum theory of angular momentum* (World Scientific, Singapore, 1988).
- [53] Robert G. Littlejohn and Matthias Reinsch, “Gauge fields in the separation of rotations and internal motions in the n-body problem,” *Rev. Mod. Phys.* **69**, 213–276 (1997).
- [54] José María Román and Joan Soto, “Effective field theory approach to ferromagnets and antiferromagnets in crystalline solids,” *International Journal of Modern Physics B* **13**, 755–789 (1999).
- [55] Christoph P. Hofmann, “Spin-wave scattering in the effective lagrangian perspective,” *Phys. Rev. B* **60**, 388–405 (1999).
- [56] O. Bär, M. Imboden, and U.-J. Wiese, “Pions versus magnons: from qcd to antiferromagnets and quantum hall ferromagnets,” *Nuclear Physics B* **686**, 347 – 376 (2004).
- [57] F. Kämpfer, M. Moser, and U.-J. Wiese, “Systematic low-energy effective theory for magnons and charge carriers in an antiferromagnet,” *Nuclear Physics B* **729**, 317 – 360 (2005).
- [58] G. P. Lepage, “How to renormalize the Schrodinger equation,” in *Nuclear physics. Proceedings, 8th Jorge Andre Swieca Summer School, Sao Jose dos Campos, Campos do Jordao, Brazil, January 26-February 7, 1997* (1997) pp. 135–180, nucl-th/9706029.
- [59] K. A. Scalfdeferri, D. R. Phillips, C.-W. Kao, and T. D. Cohen, “Short-range interactions in an effective field theory approach for nucleon-nucleon scattering,” *Phys. Rev. C* **56**, 679–688 (1997).
- [60] S.R. Beane, T.D. Cohen, and D.R. Phillips, “The potential of effective field theory in nn scattering,” *Nuclear Physics A* **632**, 445 – 469 (1998).
- [61] J. Kirscher, H. W. Griebhammer, D. Shukla, and H. M. Hofmann, “Universal correlations in pion-less eft with the resonating group method: Three and four nucleons,” *The European Physical Journal A* **44**, 239–256 (2010).
- [62] Vadim Lensky, Michael C. Birse, and Niels R. Walet, “Description of light nuclei in pionless effective field theory using the stochastic variational method,” *Phys. Rev. C* **94**, 034003 (2016).
- [63] P. Capel, D. R. Phillips, and H.-W. Hammer, “Dissecting reaction calculations using halo effective field theory and ab initio input,” *Phys. Rev. C* **98**, 034610 (2018).
- [64] Judah M. Eisenberg and Walter Greiner, *Nuclear Models: Collective and Single-Particle Phenomena* (North-Holland Publishing Company Ltd., London, 1970).
- [65] Hiroshi Kuratsuji and Shinji Iida, “Effective Action for Adiabatic Process: Dynamical Meaning of Berry and Simons Phase,” *Progress of Theoretical Physics* **74**, 439–445 (1985).
- [66] C. Alden Mead and Donald G. Truhlar, “On the determination of Born-Oppenheimer nuclear motion wave functions including complications due to conical intersections and identical nuclei,” *The Journal of Chemical Physics* **70**, 2284–2296 (1979).
- [67] Mannque Rho, “Cheshire cat hadrons,” *Physics Reports* **240**, 1 – 142 (1994).
- [68] M. Fierz, “Zur Theorie magnetisch geladener Teilchen,” *Helvetica Physica Acta* **17**, 27 (1944).
- [69] Tai Tsun Wu and Chen Ning Yang, “Dirac monopole without strings: Monopole harmonics,” *Nuclear Physics B* **107**, 365 – 380 (1976).
- [70] Jialin Zhang and T. Papenbrock, “Rotational constants of multi-phonon bands in an effective theory for deformed nuclei,” *Phys. Rev. C* **87**, 034323 (2013).
- [71] S. G. Malmskog, V. Berg, B. Fogelberg, and A. Bäcklin, “On the low-energy band structure in 187os,” *Nuclear Physics A* **166**, 573 – 593 (1971).
- [72] P. Morgen, B. S. Nielsen, J. Onsgaard, and C. Søndergaard, “The level structure of 187os,” *Nuclear Physics A* **204**, 81 – 96 (1973).
- [73] H. Sodan, W. D. Fromm, L. Funke, K. H. Kaun, P. Kemnitz, E. Will, G. Winter, and J. Berzins, “Rotational bands in 185os and 187os,” *Nuclear Physics A* **237**, 333 – 353 (1975).
- [74] Emmy Noether, “Invariante Variationsprobleme,” *Nachrichten von der Königlichen Gesellschaft der Wissenschaften zu Göttingen, Mathematisch-Physikalische Klasse* **1918**, 235–257 (1918).
- [75] André Nauts and Fabien Gatti, “Unusual commutation relations in physics,” *American Journal of Physics* **78**, 1365–1375 (2010).
- [76] H. Leutwyler, “Phonons as goldstone bosons,” *Helv. Phys. Acta* **70**, 275–286 (1997), arXiv:hep-ph/9609466 [hep-ph].
- [77] S. Weinberg, *The Quantum Theory of Fields*, Vol. II (Cambridge University Press, Cambridge, UK, 1996).
- [78] J. Gasser and H. Leutwyler, “Spontaneously broken symmetries: Effective lagrangians at finite volume,” *Nuclear Physics B* **307**, 763 – 778 (1988).

- [79] F. Wilczek and A. Shapere, *Geometric Phases in Physics* (World Scientific, Singapore, 1989) <https://www.worldscientific.com/doi/pdf/10.1142/0613>.
- [80] Shan-Tao Lai, Pancracio Palting, Ying-Nan Chiu, and Harris J. Silverstone, “On the summations involving wigner rotation matrix elements,” *Journal of Mathematical Chemistry* **24**, 123 – 132 (1998).
- [81] Tevian Dray, “A unified treatment of wigner d functions, spin-weighted spherical harmonics, and monopole harmonics,” *Journal of Mathematical Physics* **27**, 781–792 (1986).